

# The Relationship between Class I and Class II Methanol Masers

S.P. Ellingsen<sup>1</sup>

<sup>1</sup> *School of Mathematics and Physics, University of Tasmania, Private Bag 21, Hobart, Tasmania 7001, Australia;  
Simon.Ellingsen@utas.edu.au*

21 November 2018

## ABSTRACT

The Australia Telescope National Facility Mopra millimetre telescope has been used to search for 95.1-GHz class I methanol masers towards sixty-two 6.6-GHz class II methanol masers. A total of twenty-six 95.1-GHz masers were detected, eighteen of these being new discoveries. Combining the results of this search with observations reported in the literature, a near complete sample of sixty-six 6.6-GHz class II methanol masers has been searched in the 95.1-GHz transition, with detections towards 38 per cent (twenty-five detections ; not all of the sources studied in this paper qualify for the complete sample, and some of the sources in the sample were not observed in the present observations).

There is no evidence of an anti-correlation between either the velocity range, or peak flux density of the class I and II transitions, contrary to suggestions from previous studies. The majority of class I methanol maser sources have a velocity range that partially overlaps with the class II maser transitions. The presence of a class I methanol maser associated with a class II maser source is not correlated with the presence (or absence) of main-line OH or water masers. Investigations of the properties of the infrared emission associated with the maser sources shows no significant difference between those class II methanol masers with an associated class I maser and those without. This may be consistent with the hypothesis that the objects responsible for driving class I methanol masers are generally not those that produce main-line OH, water or class II methanol masers.

**Key words:** masers – stars:formation – ISM: molecules – radio lines : ISM

## 1 INTRODUCTION

Intense activity in the field of methanol maser research commenced in the mid 1980s with the discovery of numerous new transitions (e.g. Morimoto et al. 1985; Wilson et al. 1984, 1985, and others). As the number of methanol maser transitions increased it became clear that they could be classified empirically into two groups on the basis of the sources towards which they were detected (Batra et al. 1987; Menten 1991a). Class II methanol masers are found close to sites of high-mass star formation and are often associated with HII regions, infrared sources and OH masers. The strongest and most widespread class II transitions are the  $5_1 - 6_0A^+$  (6.6 GHz) and  $2_0 - 3_{-1}E$  (12.1 GHz), which have been detected towards more than 500 sites within the Galaxy (Pestalozzi, Minier & Booth 2004, and references therein). The archetypal class II methanol maser source is W3(OH). Class I methanol masers are also found towards star formation regions, but offset by small, though significant amounts from HII regions, infrared sources, OH

and water masers. The strongest class I transitions are the  $7_0 - 6_1A^+$  (44.0 GHz) and  $4_{-1} - 3_0E$  (36.1 GHz), and the archetypal source is Orion KL. The class II  $2_0 - 3_{-1}E$  transition is often observed in absorption towards class I sources (Peng & Whiteoak 1992). Theoretical models of methanol masers provide some explanation for this empirical division predicting inversion in the class I transitions when collisional processes dominate and inversion in the class II transitions when radiative processes dominate (Cragg et al. 1992; Sobolev & Deguchi 1994; Sobolev, Cragg & Godfrey 1997).

The classification suggested by Menten (1991a) was consistent with the observational and theoretical understanding at the time. However, more recent studies suggest that things may be more complicated. A number of searches for class I methanol masers have been made towards traditional class II sites with relatively high detection rates (Slysh et al. 1994; Val'tts et al. 2000). Slysh et al. (1994) suggested an anti-correlation between the intensities and velocity ranges of the class I and II methanol masers

within the same region. This requires that there is some sort of relationship between the emission from the two transitions since, if they were independent neither correlations, nor anti-correlations should exist. Perhaps more importantly, modelling predicts that in some conditions the 6.6-GHz class II transition can be weakly inverted, simultaneously with strong inversion in the 25-GHz class I transitions. This situation may have recently been detected towards the archetypal class I maser source Orion KL (Voronkov et al. 2004). Kurtz, Hofner & Álvarez (2004) found coincidence within 0.5 arcsec of class I and II methanol masers in one source, although there is a significant velocity difference between the two transitions suggesting that it may be a chance alignment along our line of sight.

The majority of studies of methanol masers have focused upon the class II transitions. There are two main reasons for this ; the first is that the strongest class II transitions are in the centimetre regime and hence easier to observe ; the second is that their association with other maser species, *IRAS* sources etc makes targeted searches relatively productive (e.g. Menten 1991b; Caswell et al. 1995b; Walsh et al. 1997). Although untargeted searches have also been very successful at detecting class II methanol masers (Caswell 1996; Ellingsen et al. 1996; Szymczak et al. 2002). In contrast the strongest class I methanol maser transitions are at millimetre wavelengths and to date there is no other type of astrophysical object with which they are known to be closely associated. Menten (1991a) suggested that class I masers are offset from class II sites by up to 1 pc. However, there are relatively few sources where both class I and II transitions have been imaged at high resolution. The majority of the well studied class I methanol maser sources are “traditional” class I sources with no (or weak) class II emission, Orion KL (Plambeck & Wright 1988; Johnston et al. 1992), DR21 (Batra & Menten 1988; Plambeck & Menten 1990) and Sgr B2 (Mehringer & Menten 1997). There are no strong class II methanol masers towards Orion KL, although weak masers, and possibly quasi-thermal emission has been detected Voronkov et al. (2004). There is class II methanol maser emission towards DR21(OH), this likely to be from the same region as the OH maser emission (which is offset from the class I masers), but this has not been confirmed. Sgr B2 is a very complex region, with multiple site of both class I and II methanol masers. The class II masers are close to the compact HII regions Houghton & Whiteoak (1995), while the majority of class I masers lie in an arc, possibly tracing the interface between two molecular clouds Mehringer & Menten (1997).

For a source at a distance of 3 kpc (typical for a high-mass star forming region) a linear distance of 1 pc corresponds to an angular separation of slightly more than 1 arcminute. This is comparable to, or larger than typical telescope beam sizes at millimetre wavelengths and so searches targeted at class II maser sites (e.g. Slysh et al. 1994; Val’tts et al. 2000) would be expected to detect few class I sources. This is not the case though, which suggests that in many cases the offset between class I and II maser sites is significantly less than 1 pc. This has been confirmed by recent VLA observations of 44 GHz class I methanol masers (Kurtz et al. 2004) which found a median separation of 0.2 pc from HII regions. At the present time, class II methanol maser sites appear to be the best targets for class I

maser searches. However, the nature of the relationship between the two classes remains unclear. To try and elucidate the nature of the relationship I have undertaken a search for class I methanol masers towards a statistically complete sample of class II methanol masers selected from the Mt Pleasant survey (Ellingsen et al. 1996; Ellingsen 1996).

## 2 OBSERVATIONS AND DATA REDUCTION

The observations were made between 1998 July 12–17 using the Australia Telescope National Facility (ATNF) 22m millimetre antenna at Mopra. At the time of the observations only the inner 15 m of the Mopra antenna was illuminated and the antenna had a sensitivity of approximately 40 Jy K<sup>-1</sup>. The assumed rest frequency of the 8<sub>0</sub> – 7<sub>1</sub>A<sup>+</sup> was 95.169 489 GHz (De Lucia et al. 1989) and at this frequency the half-power beam width of the Mopra antenna was 52 arcsec. Recent measurement of the rest frequencies of various methanol maser transitions by Müller, Menten & Mäder (2004) gives a value of 95.169 463 GHz (with an uncertainty of 10 kHz). This is 14 kHz lower than the value used, which means that the velocities listed are 0.044 km s<sup>-1</sup> higher than had the more recent rest frequency value been used. The data were collected using a 2-bit digital autocorrelation spectrometer configured with 1024 channels spanning a 32-MHz bandwidth. For an observing frequency of 95.1 GHz this configuration yields a natural weighting velocity resolution of 0.12 km s<sup>-1</sup>, or 0.2 km s<sup>-1</sup> after Hanning smoothing. The SIS mixers on both of the available linear polarization channels were tuned to the 95.1 GHz methanol transition. The antenna pointing was checked and corrected prior to each observing session by making observations of 86-GHz SiO masers; the nominal pointing accuracy is of the order of 10 arcsec RMS. For one of the channels the tuning was performed only once at the beginning of the observing period. However, the other channel had to be retuned each day after the pointing checks. The sensitivity of this channel varied day to day depending upon how well the receiver tuned, in general it had a system temperature approximately 50K higher than the other channel, though on occasions it was slightly lower. The system temperature was determined by inserting an ambient temperature load which was assumed to have a temperature of 295K. The measured system temperature varied between 200 and 340K depending upon the weather conditions and elevation. This method of calibration also corrects for atmospheric absorption (Kutner & Ulich 1981) and taking into account pointing inaccuracies the absolute accuracy of the flux density scale of the observations is conservatively estimated to be 20 per cent. The sources were observed in a position switching mode with 300 seconds spent at the on-source position and 300 seconds at a reference position offset in declination 30 arcminutes to the south. This procedure was repeated 3 times to yield a total on-source integration time of 15 minutes for most sources, which typically yielded an RMS of 1.3 Jy after averaging the two polarizations and Hanning smoothing. Wiesemeyer, Thum & Walmsley (2004) recently observed linear polarization in excess of 10% in a number of class I methanol maser transitions, including the 95.1-GHz. The spectra presented here are an average of two orthogonal linear polarizations and hence the relative flux density of

the features will not be effected by any linear polarization. The current observations were made in such a way that it is not possible to determine the polarization characteristics of the masers from them. The data were processed using the SPC reduction package. Quotient spectra were formed for each on/off pair of observations which were then averaged together, a polynomial baseline fitted and subtracted and the velocity and amplitude scale calibrated. Velocity calibration presented some challenges, requiring correction for incorrectly recorded frequency synthesiser chain information in the RPFITS header Ladd et al. (2004) and editing of the telescope identity and band-inversion in the headers.

The sample of 6.6-GHz methanol maser sites searched for 95.1-GHz maser emission was drawn from Ellingsen et al. (1996) and Ellingsen (1996) and included all sources detected in the regions with Galactic longitude  $l = 25^\circ - 30^\circ, 282^\circ - 286^\circ, 291^\circ - 296^\circ, 325^\circ - 335^\circ$ . For the first and last of these longitude ranges the Galactic latitude range of the Mt Pleasant survey was  $b = -0^\circ.53 - +0^\circ.53$ , while for the other regions it was  $b = -1^\circ.03 - +0^\circ.03$ . The total area covered is approximately 24.4 square degrees. The exact number of class II methanol masers sites within these regions depends on the spatial resolution of the observations. A number of the sources have two or more sites of emission separated by a few arcseconds. Such sources cannot be resolved with the Mopra telescope and so in general we have made observations towards individual sites only where they are separated by more than 20 arcsec. Observations of the 95.1-GHz transition were made of a small number of sources not detected as part of the original Mt Pleasant survey. In particular, 326.475+0.703 which was listed as 326.40+0.51 in the original survey (Ellingsen et al. 1996), the correct position being revealed by Australia Telescope Compact Array (ATCA) observations. 27.286+0.151 is outside the velocity range of the Mt Pleasant survey, but was discovered during ATCA observations of the nearby source 27.223+0.137. In addition, the untargeted search of Caswell (1996) detected a number of 6.6-GHz methanol masers in the region  $l = 330^\circ - 335^\circ$  which were not detected in the Mt Pleasant survey either due to variability or being outside the searched velocity range (331.120–0.118, 333.029–0.063, 333.646+0.058 & 334.935–0.098) and these were also searched for 95.1-GHz methanol masers. An independent untargeted survey of the  $l = 20^\circ - 40^\circ$  region has recently been undertaken with the Torun telescope (Szymczak et al. 2002), which also discovered a number of sources in the  $l = 25^\circ - 30^\circ$  region not detected at Mt Pleasant. However these were not searched as the information was not available at the time of the observations. For the majority of sources (80 of 84) the positions search for 95.1-GHz class I methanol masers are the sites of class II masers determined from ATCA observations which have a positional accuracy of approximately 0.5 arcsec (Ellingsen, unpublished observations). The only exceptions were the sources 285.32–0.03, 293.84–0.78, 293.95–0.91 and 25.53+0.38, for which the positions determined in the Mt Pleasant survey (positional accuracy RMS 0.6 arcmin) were used (Ellingsen et al. 1996). For those sources where ATCA position are available we have used three significant figures for the Galactic coordinate names. These names differ slightly from those used previously in the literature, but the greater accuracy of the ATCA positions warrants it, and the correspondence is in most cases reasonably obvious.

A small number of the detected 95.1-GHz methanol masers were either not observed, or have poor spectra from the original 6.6-GHz Mt Pleasant survey. To enable proper comparison of the class I and class II emission in all class I detections, new 6.6-GHz observations were made of the sources 326.474+0.703, 333.029–0.063 and 27.286+0.151. These observations were made with the Mt Pleasant 26-m telescope on 2004 November 3 & 8. The assumed rest frequency of the  $5_1-6_0A^+$  transition was 6.668518 GHz, and at this frequency the half-power beam width of the Mt Pleasant antenna is 7 arcmin. The observations were made with a cryogenically cooled receiver with dual circular polarizations and a system equivalent flux density of approximately 1200 Jy. The data were collected using a 2-bit autocorrelation spectrometer configured with 4096 channels spanning a 4-MHz bandwidth for each polarizations. For an observing frequency of 6.6-GHz this configuration yields a velocity resolution after Hanning smoothing of  $0.09 \text{ km s}^{-1}$ . Each source was observed in position switching mode with 10 minutes spent at the on-source position and a further 10 minutes at a reference position offset by -1 degree in declination. To measure any pointing errors a 5-point grid, centred on the nominal position was observed for each source. In each case the measured pointing offsets were small, implying scaling corrections to the flux density scale of the source spectra of less than 5 per cent. As this is less than the accuracy of the flux density calibration, no scaling was applied.

### 3 RESULTS

A total of fifty-nine 6.6-GHz class II methanol maser sites were searched for 95.1 GHz class I masers. Emission was detected towards twenty-six sites and these are listed, along with the parameters of Gaussian fits to the emission in Table 1. Spectra of each of the detected 95.1-GHz masers are shown in Figure 1. Eighteen of the 95.1-GHz emission sites detected are new discoveries, with the remainder previously observed by Val'tts et al. (2000). The sources for which no emission was detected are listed in Table 2, along with the velocity range searched and the  $3\sigma$  detection limit for the observation.

The primary purpose of these observations was to realise a search for 95.1-GHz class I methanol masers towards a statistically complete sample of 6.6-GHz class II methanol masers. Table 3 gives the intensity and velocity of the peak flux density and the velocity range for both the class I and class II methanol masers for all the 6.6-GHz masers detected in the Mt Pleasant survey (not just those in the statistically complete sample) and the additional sources listed in section 2. There are two 6.6-GHz class II methanol maser sources from the statistically complete sample which were accidentally omitted from the sources searched for 95.1-GHz class I masers (328.254–0.254 & 28.201–0.049). The data for the class II emission in these sources is included in Table 3. Fortunately the omission of two of sixty-eight sources does not significantly effect the reported statistics or conclusions of this study. For sources where both classes of methanol maser were detected spectra of each are shown on a common velocity scale in Figure 1. Many of the class II methanol maser spectra contain emission from multiple sources, present within a single Mt Pleasant beam (7

**Table 1.** Class II methanol maser sites detected in the 95.1-GHz class I transition. The Hanning smoothed spectra have been fitted with one or more Gaussian profiles and the fitted parameters are listed, the number in brackets is the uncertainty reported by the fitting procedure. Notes : <sup>a</sup> sources not within the statistically complete sample of 6.6-GHz methanol masers.

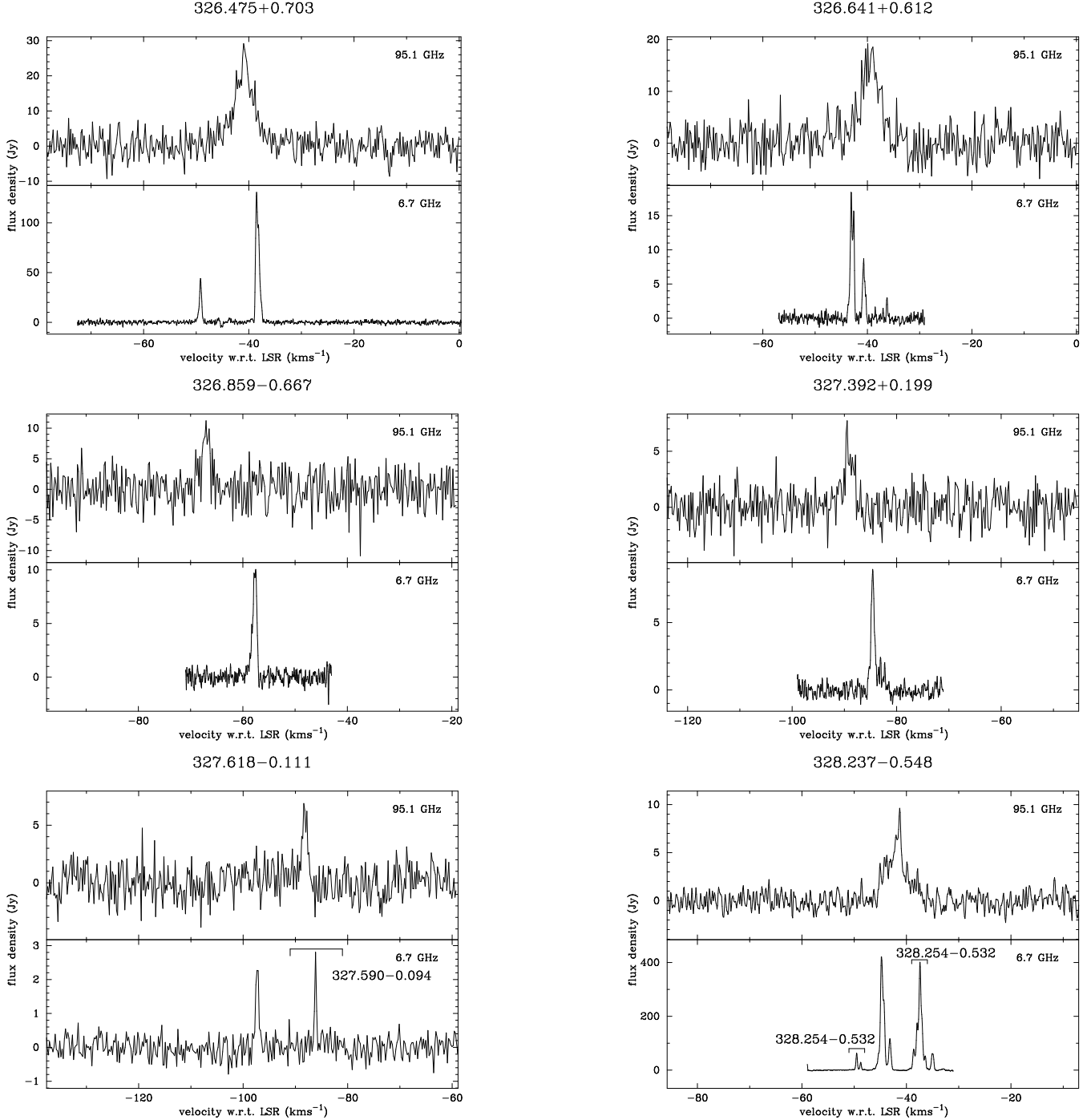
Name	Right Ascension (J2000) (h m s)	Declination (J2000) (° ' ")	Peak Flux Density (Jy)	Velocity (km s <sup>-1</sup> )	Full Width Half Maximum (km s <sup>-1</sup> )
328.237−0.548 <sup>a</sup>	15:57:58.381	-53:59:23.14	5.2(1.3)	-41.8(0.1)	1.6(0.3)
			4.4(0.8)	-41.3(0.05)	0.4(0.1)
			3.8(0.5)	-44.0(0.2)	2.2(0.3)
			2.3(0.4)	-39.7(0.9)	3.9(1.3)
328.809+0.633 <sup>a</sup>	15:55:48.608	-52:43:06.20	18.3(1.6)	-40.9(0.1)	1.5(0.1)
			17.3(1.4)	-41.4(0.05)	5.2(0.2)
			14.1(1.2)	-40.5(0.05)	0.4(0.05)
			13.9(1.1)	-42.6(0.05)	1.3(0.1)
329.031−0.198	16:00:30.326	-53:12:27.35	13.4(1.0)	-47.0(0.05)	0.7(0.1)
			12.0(1.9)	-43.9(0.1)	1.3(0.2)
			8.0(0.5)	-46.0(0.2)	2.4(0.3)
			6.7(2.4)	-43.5(0.1)	1.2(0.3)
			5.7(2.0)	-43.7(0.05)	0.4(0.2)
331.132−0.244	16:10:59.743	-51:50:22.70	4.4(0.6)	-41.6(0.6)	4.4(0.9)
			31.6(0.6)	-91.1(0.05)	0.8(0.05)
			8.8(0.7)	-88.5(0.05)	0.5(0.1)
			8.4(0.2)	-86.7(0.1)	6.9(0.2)
			5.6(0.6)	-84.6(0.05)	0.8(0.1)
331.342−0.346	16:12:26.456	-51:46:16.86	12.9(0.7)	-65.8(0.05)	0.6(0.05)
332.295−0.094	16:15:45.381	-50:55:53.85	14.5(5.4)	-50.8(0.05)	0.5(0.1)
332.942−0.686 <sup>a</sup>	16:21:19.018	-50:54:10.41	4.6(0.4)	-48.6(0.1)	3.6(0.3)
			3.8(0.7)	-49.0(0.1)	0.7(0.2)
332.963−0.679 <sup>a</sup>	16:21:22.926	-50:52:58.71	9.1(0.7)	-46.8(0.05)	0.6(0.1)
			8.5(1.0)	-47.4(0.05)	0.5(0.1)
			3.0(0.3)	-49.0(0.2)	4.4(0.5)
333.029−0.063 <sup>a</sup>	16:18:56.735	-50:23:54.17	3.7(1.0)	-41.0(0.1)	0.4(0.1)
			2.8(0.5)	-40.1(0.1)	1.0(0.3)
			6.1(0.2)	-50.9(0.1)	7.1(0.2)
333.121−0.434	16:20:59.704	-50:35:52.32	6.0(0.5)	-52.9(0.05)	0.9(0.1)
			5.3(0.7)	-50.7(0.05)	0.4(0.1)
			23.3(0.7)	-47.6(0.05)	2.7(0.1)
333.128−0.440	16:21:03.300	-50:35:49.75	21.9(1.2)	-48.6(0.05)	1.2(0.1)
			9.2(0.8)	-49.9(0.1)	2.0(0.2)
			7.4(0.4)	-50.6(0.2)	7.1(0.4)
			7.6(0.6)	-59.1(0.05)	1.4(0.1)
333.130−0.560 <sup>a</sup>	16:21:35.742	-50:40:51.29	6.4(0.6)	-54.4(0.05)	0.5(0.1)
			4.6(0.2)	-56.5(0.2)	3.8(0.4)
			3.7(0.5)	-91.3(0.05)	0.6(0.1)
333.163−0.101 <sup>a</sup>	16:19:42.670	-50:19:53.20	3.5(0.7)	-109.8(0.05)	0.5(0.1)
			4.4(1.8)	-87.0(0.1)	0.2(0.2)
333.184−0.091	16:19:45.620	-50:18:35.00	4.3(0.8)	-86.5(0.1)	1.4(0.3)
			131.9(0.9)	-87.3(0.05)	1.1(0.05)
333.234−0.062	16:19:51.250	-50:15:14.10	17.7(0.8)	-87.6(0.05)	4.0(0.1)
			2.5(0.3)	-46.5(0.3)	3.5(0.8)
333.315+0.105	16:19:29.016	-50:04:41.45	2.2(0.8)	-44.4(0.2)	1.0(0.5)
			7.5(0.4)	-42.9(0.1)	3.0(0.2)
333.466−0.164	16:21:20.180	-50:09:48.60	5.1(0.7)	-45.2(0.05)	0.5(0.1)
			4.7(0.8)	-42.8(0.05)	0.4(0.1)
			11.8(1.6)	-40.0(0.1)	0.6(0.1)
333.562−0.025	16:21:08.797	-49:59:48.26	6.7(1.9)	-39.4(0.1)	0.6(0.2)
			4.3(1.5)	-40.1(0.2)	2.1(0.4)
			2.9(0.5)	-39.3(0.1)	2.9(0.4)
335.060−0.427 <sup>a</sup>	16:29:23.146	-49:12:27.34	1.7(0.8)	-39.2(0.1)	0.4(0.3)
			53.8(1.0)	90.2(0.05)	0.4(0.05)
25.826−0.178	18:39:03.621	-06:24:09.29	15.4(1.0)	98.4(0.05)	0.7(0.05)
			10.0(1.0)	91.7(0.05)	0.3(0.05)
			9.8(0.4)	94.2(0.1)	4.3(0.3)
			4.6(0.7)	91.4(0.1)	2.5(0.3)
			1.7(0.9)	98.5(0.4)	1.4(0.9)
26.602−0.220	18:40:38.550	-05:43:56.20	8.3(1.6)	108.0(0.05)	0.3(0.1)
			2.8(0.7)	106.8(0.2)	1.0(0.6)

Table 1 – *continued*

Name	Right Ascension (J2000) (h m s)	Declination (J2000) (° ' ")	Peak Flux Density (Jy)	Velocity (km s <sup>-1</sup> )	Full Width Half Maximum (km s <sup>-1</sup> )	Ref
27.286+0.151 <sup>a</sup>	18:40:34.476	-04:57:13.44	3.6(0.4)	31.6(0.05)	0.8(0.1)	*
			3.1(0.5)	33.1(0.05)	0.5(0.1)	
27.369-0.164	18:41:50.982	-05:01:28.23	22.9(0.8)	95.3(0.05)	0.5(0.05)	*
			20.2(0.9)	93.7(0.1)	1.8(0.1)	
			13.7(1.4)	94.2(0.05)	0.5(0.1)	
			6.2(0.4)	92.0(0.1)	7.0(0.3)	
			5.8(0.6)	90.6(0.05)	0.6(0.1)	
			4.1(0.7)	92.1(0.05)	0.4(0.1)	
28.303-0.389	18:44:22.056	-04:17:48.84	4.7(1.0)	74.0(0.05)	0.2(0.1)	*
29.907-0.040	18:46:03.585	-02:42:36.34	26.6(1.0)	98.2(0.05)	0.3(0.05)	*
29.974-0.029	18:46:08.505	-02:38:42.66	3.1(0.6)	96.4(0.1)	0.5(0.2)	1
			2.2(0.8)	97.0(0.1)	0.4(0.2)	

**Table 2.** Class II methanol maser sites not detected in the 95.1-GHz class I transition. The RMS noise level listed is that measured in the Hanning smoothed spectra. Notes : <sup>a</sup> sources not within the statistically complete sample of 6.6-GHz methanol masers, <sup>b</sup> emission detected towards this source, but it appears to be a sidelobe response to 29.907-0.040.

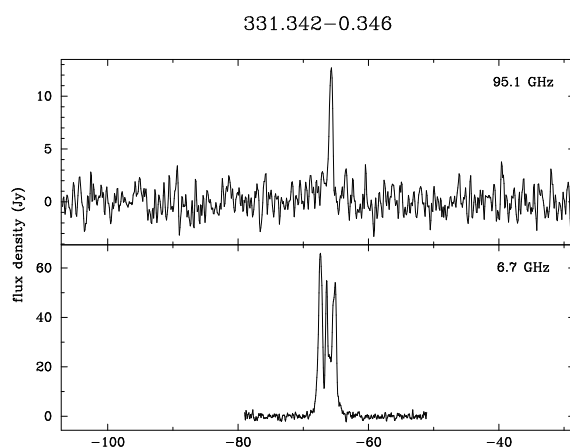
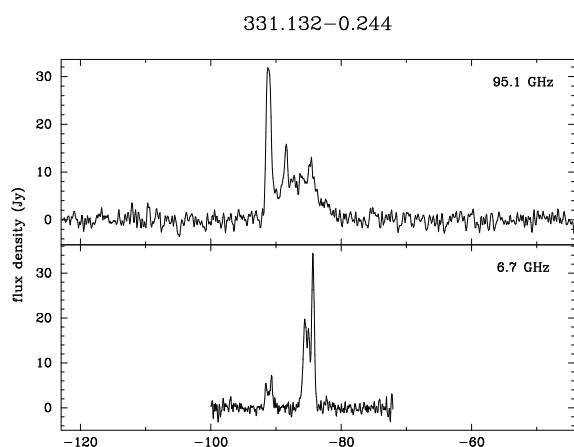
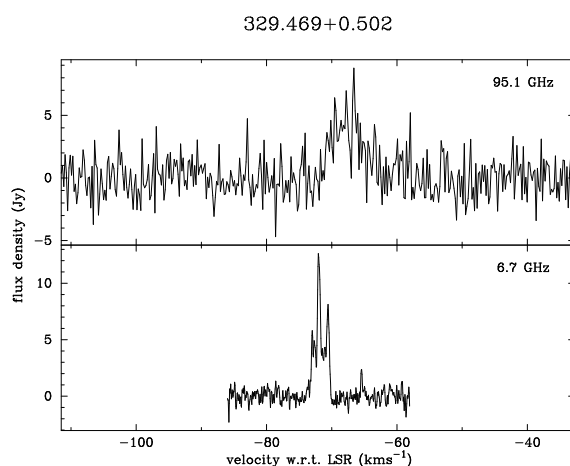
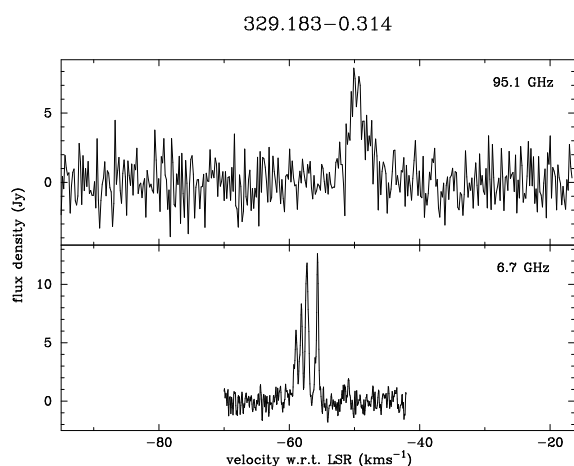
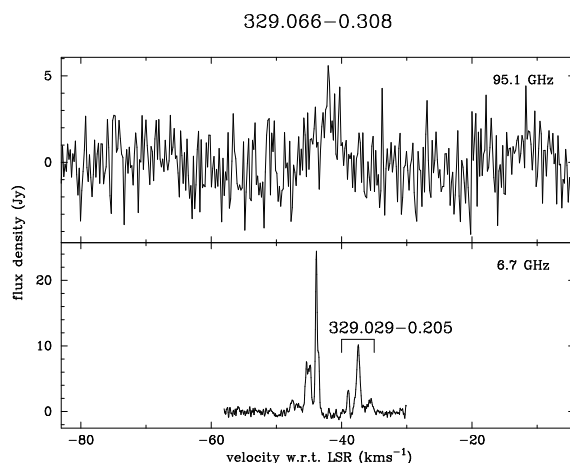
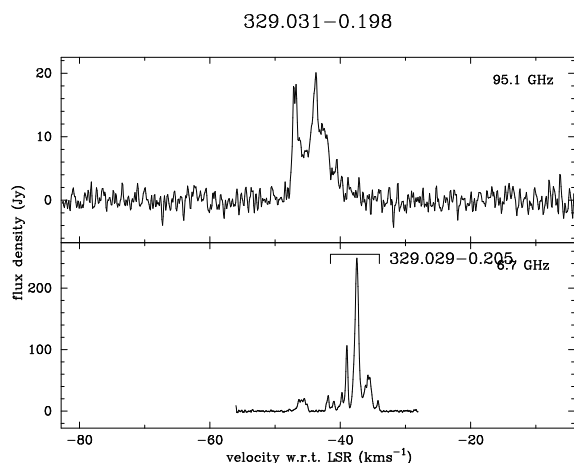
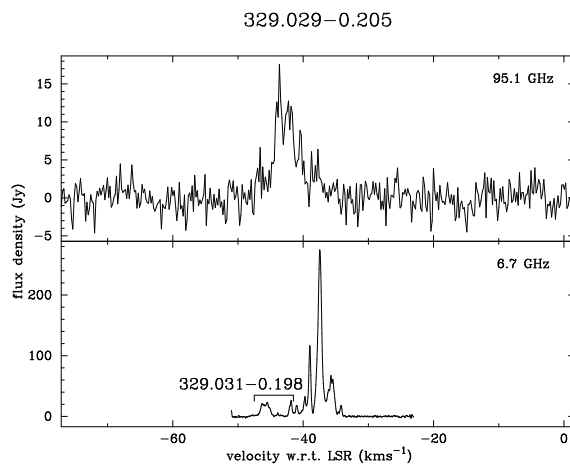
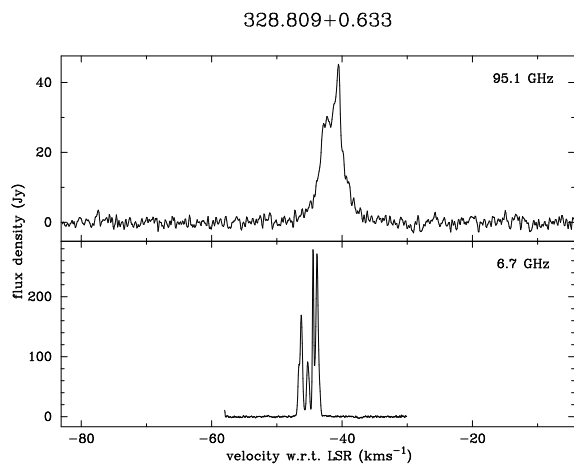
Name	R.A.(J2000) (h m s)	Dec.(J2000) (° ' ")	Velocity Range (km s <sup>-1</sup> )	3 $\sigma$ (Jy)
327.120+0.511	15:47:32.729	-53:52:38.90	-120 – -55	4.4
327.401+0.445	15:49:19.4	-53:45:14	-122 – -46	4.2
327.402+0.444	15:49:19.523	-53:45:14.21	-122 – -46	4.2
327.590-0.094	15:52:36.824	-54:03:18.97	-122 – -46	4.8
329.407-0.459	16:03:32.662	-53:09:26.98	-105 – -29	4.2
330.952-0.182 <sup>a</sup>	16:09:52.372	-51:54:57.89	-127 – -50	4.2
331.278-0.188	16:11:26.596	-51:41:56.67	-118 – -40	3.8
331.542-0.066	16:12:09.020	-51:25:47.60	-124 – -47	3.8
331.556-0.121 <sup>a</sup>	16:12:27.210	-51:27:38.20	-143 – -66	4.1
333.029-0.015	16:18:44.167	-50:21:50.77	-92 – -16	3.0
333.068-0.447	16:20:48.995	-50:38:40.72	-92 – -16	3.4
333.646+0.058 <sup>a</sup>	16:21:09.140	-49:52:45.90	-127 – -50	3.8
333.683-0.437	16:23:29.794	-50:12:08.69	-45 – 32	3.3
333.931-0.135	16:23:14.831	-49:48:48.87	-76 – 0	4.1
334.635-0.015	16:25:45.729	-49:13:37.51	-70 – 7	3.2
334.935-0.098 <sup>a</sup>	16:27:24.250	-49:04:11.30	-67 – 20	3.0
25.411+0.105	18:37:16.918	-06:38:28.23	58 – 136	4.2
25.386+0.005	18:37:35.522	-06:42:34.34	56 – 132	3.9
25.53+0.38	18:36:32.6	-06:24:26	52 – 130	3.7
25.710+0.044	18:38:03.097	-06:24:14.31	56 – 132	4.1
26.528-0.266	18:40:40.227	-05:49:07.67	66 – 142	4.0
27.223+0.137	18:40:30.434	-05:00:58.88	80 – 156	3.0
28.151-0.002	18:42:42.494	-04:15:18.34	62 – 138	3.1
28.829+0.488	18:42:12.433	-03:25:39.56	46 – 122	3.2
28.863-0.237	18:44:51.000	-03:43:44.17	50 – 126	3.3
28.810+0.360	18:42:37.485	-03:30:12.52	56 – 130	3.4
29.313-0.165	18:45:24.974	-03:17:44.47	6 – 82	3.4
29.867-0.042	18:45:59.530	-02:44:47.23	56 – 132	3.5
29.865-0.007	18:45:51.765	-02:43:57.38	52 – 128	3.5
29.895-0.047 <sup>b</sup>	18:46:03.653	-02:43:24.89	60 – 136	3.1
29.918-0.035 <sup>b</sup>	18:46:03.690	-02:41:52.53	60 – 136	2.9
29.923+0.059	18:45:44.184	-02:39:03.71	60 – 136	3.1
30.009-0.017	18:46:09.851	-02:36:30.75	60 – 136	3.4

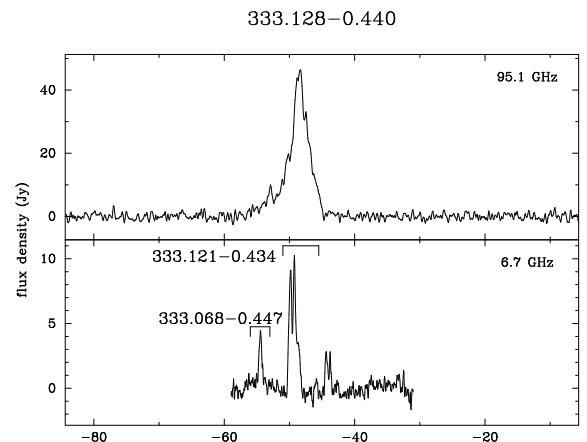
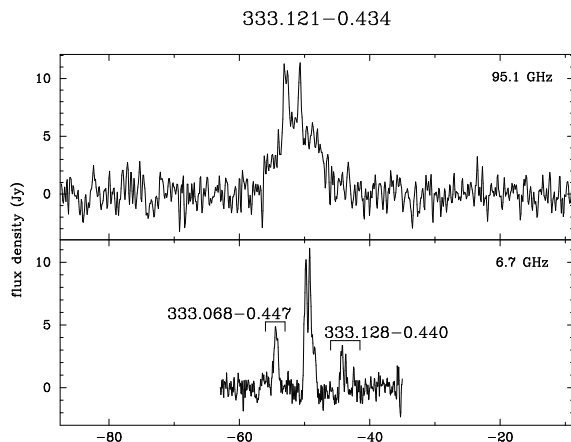
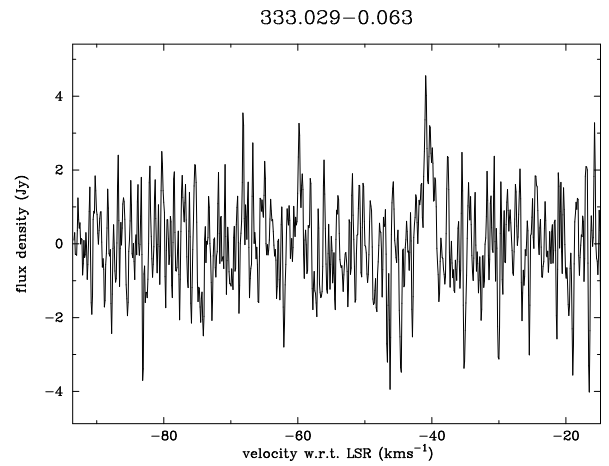
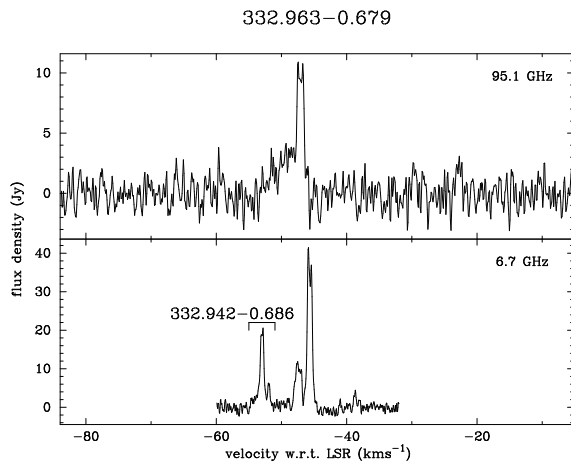
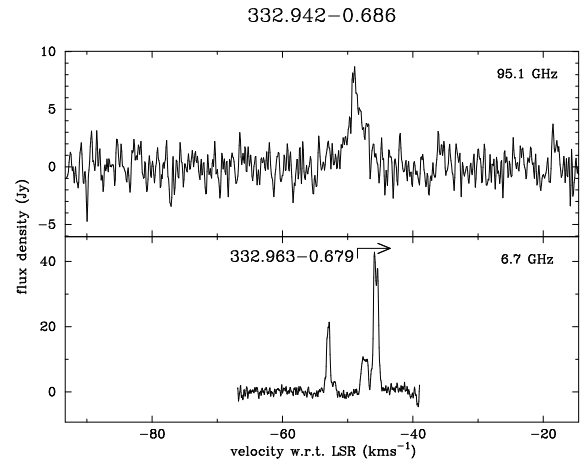
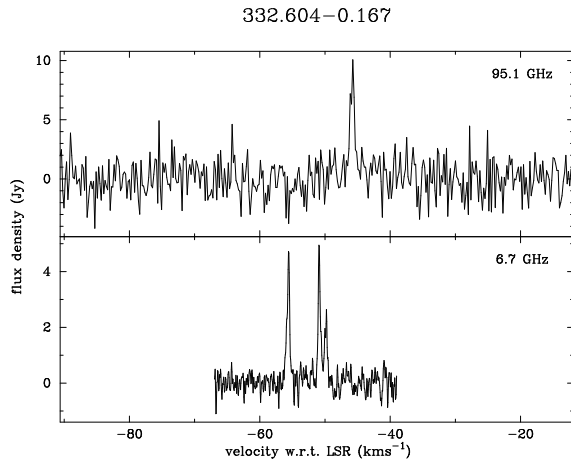
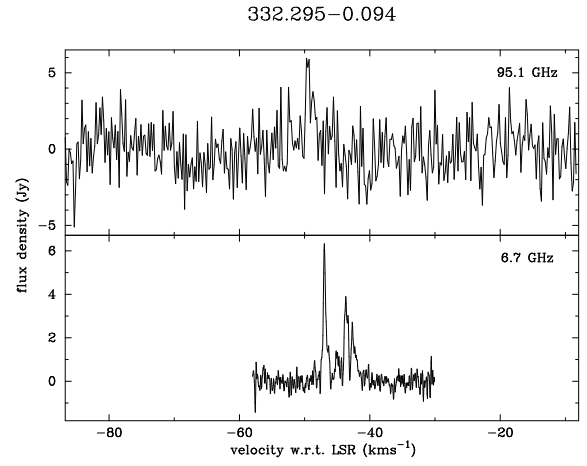
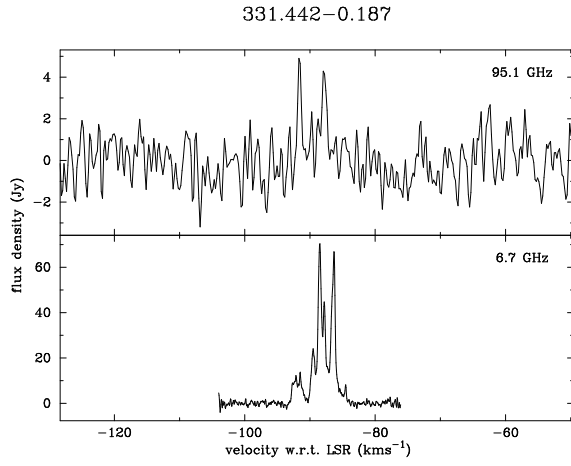


**Figure 1.** Spectra of the 95.1-GHz class I methanol maser sources (top) and the corresponding 6.6-GHz class II methanol masers (bottom). The 95.1-GHz spectra are from the current work, except for those sources where Val'tts et al. (2000) is the only reference listed in Table 3. The 6.6-GHz spectra are from either Ellingsen et al. (1996), Ellingsen (1996) or the current work, as listed in the relevant column of Table 3. All 95.1-GHz spectra have been Hanning smoothed.

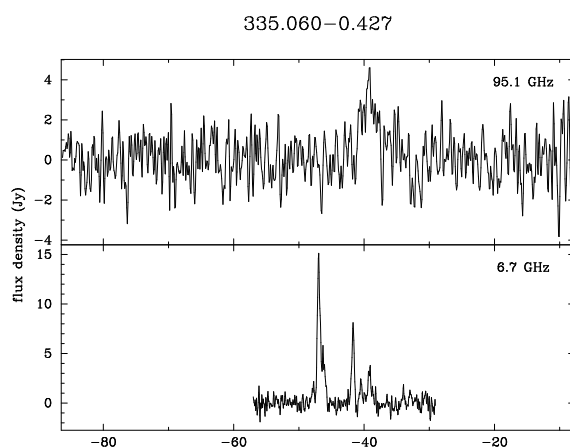
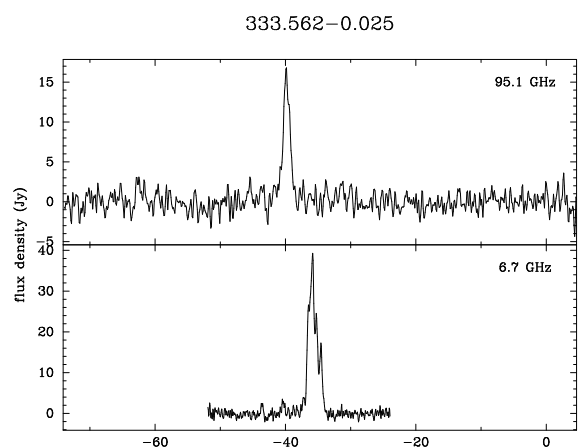
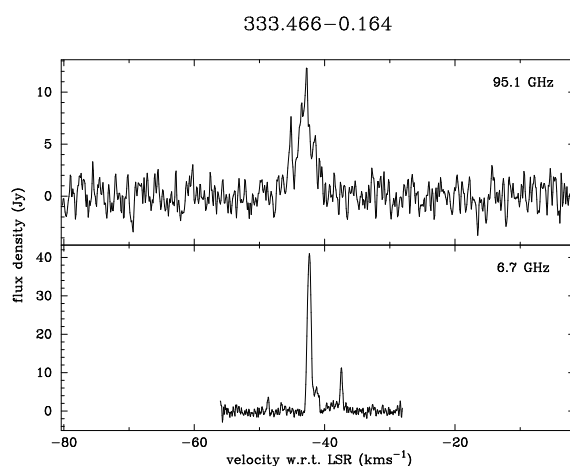
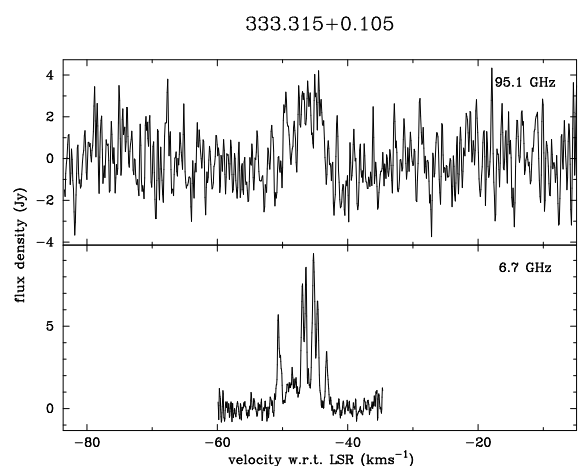
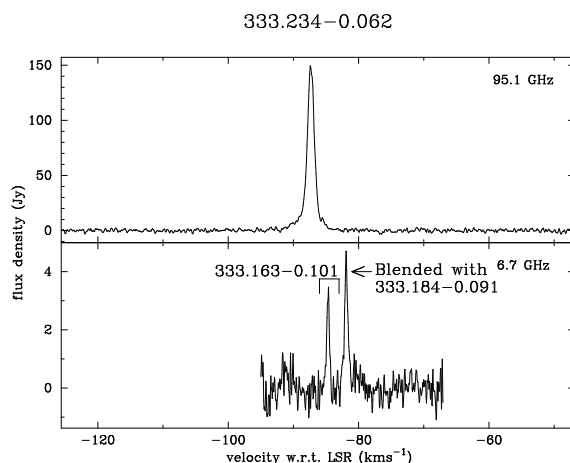
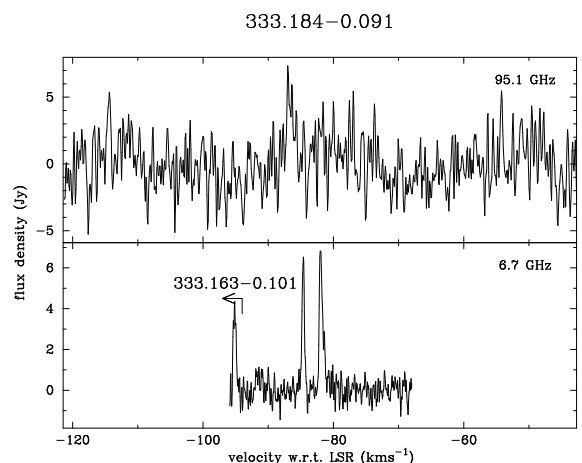
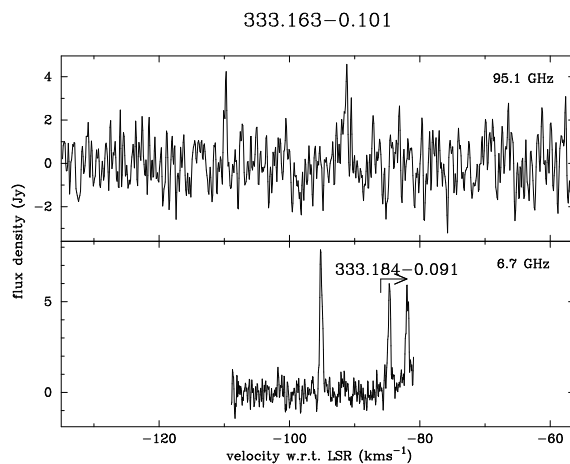
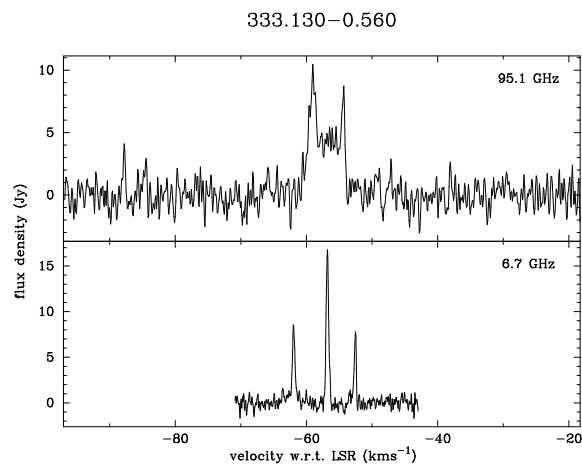
arcmin at 6.6 GHz). Where this occurs the emission from the nearby sources is indicated in the spectra. Examination of Fig. 1 shows that the peaks of the two classes of methanol masers essentially never coincide in velocity. The median difference between the peak velocity of the class I and class II transitions is 3.6 km s<sup>-1</sup> (Fig. 2). This is less than the median velocity width (5 km s<sup>-1</sup>) for the class II methanol

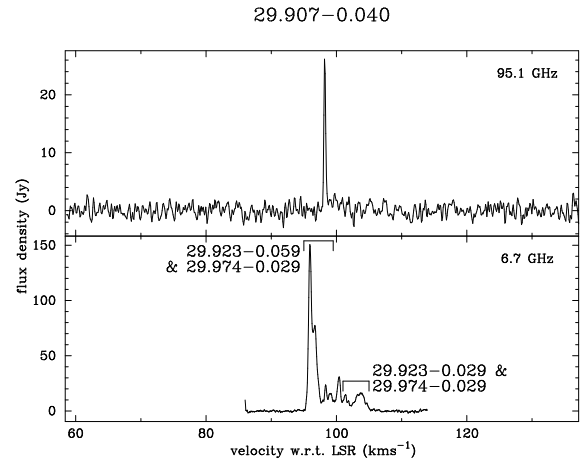
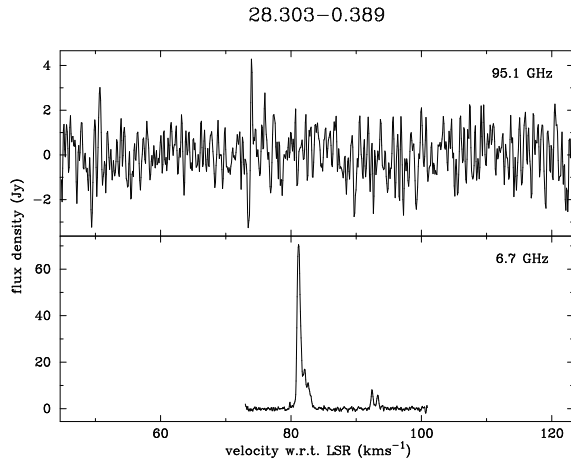
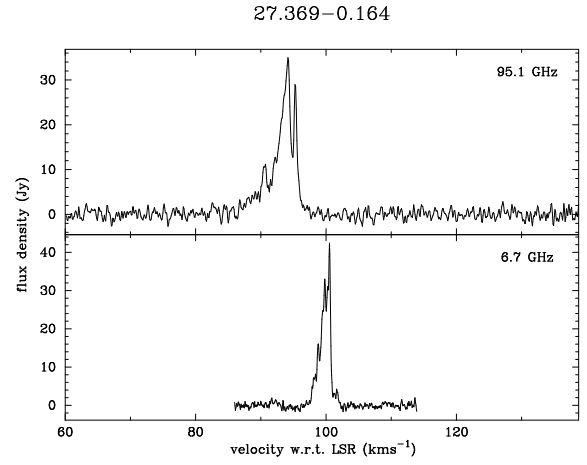
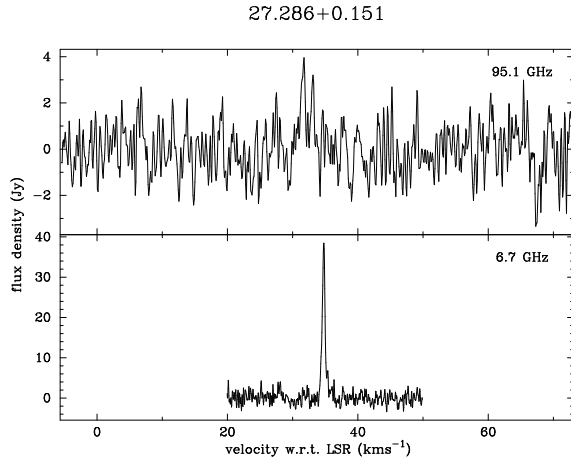
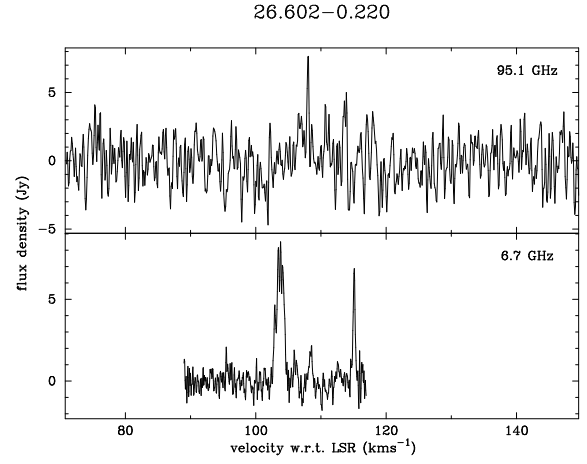
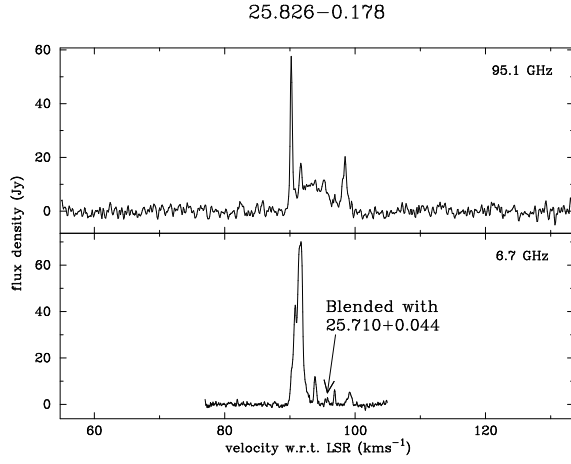
masers with associated class I emission, suggesting a significant degree of overlap exists between the velocity ranges of the two classes. This can be examined directly by investigating the minimum separation of the velocity ranges between the class I and II emission (Figure 3). The separation here is defined to be the difference between the lowest velocity of the class with the larger mean velocity, and the highest ve-



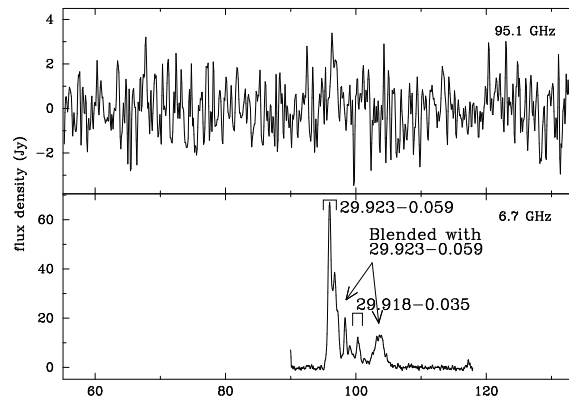








29.974–0.029



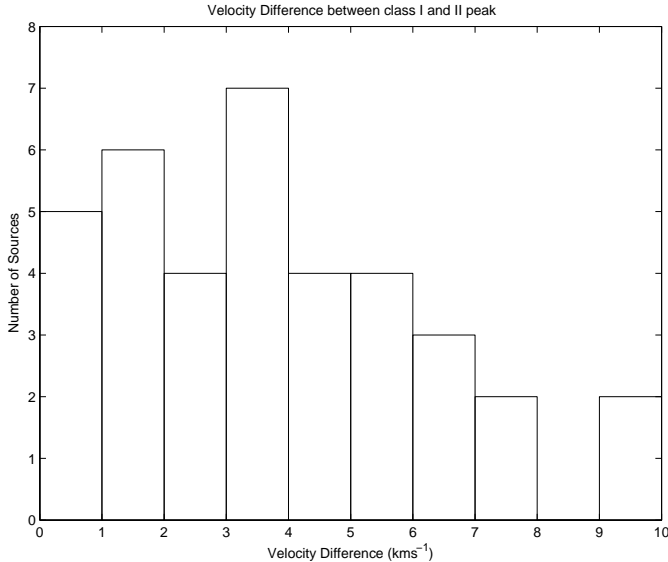


**Figure 2.** The difference between the peak velocity of the class I 95.1-GHz methanol masers and the corresponding class II 6.6-GHz transition

locity of the class with the lower mean velocity. For example for 326.475+0.703 the class I masers cover a velocity range from  $-43 - -38 \text{ km s}^{-1}$  (a mean velocity of  $-40.5 \text{ km s}^{-1}$ ), while the class II masers have a velocity range from  $-51 - -37 \text{ km s}^{-1}$  (a mean velocity of  $-44 \text{ km s}^{-1}$ ), so the class I masers have the higher mean velocity and the separation is  $-43 - -37 = -6 \text{ km s}^{-1}$ . A negative value in Fig. 3 indicates overlapping velocity ranges and a positive value, non-overlapping velocity ranges. The median separation observed in the sample is  $-2 \text{ km s}^{-1}$ , i.e. more than 50 per cent of sources show an overlap in the velocity ranges of the two classes. This is contrary to the suggestion of Slysh et al. (1994) who claim an anti-correlation between the velocities of the two classes. Fig. 3 shows that in the majority of cases (23 of 37) there is an overlap in the velocity ranges and sometimes the overlap is large.

Figure 1 shows that there are significant differences in the typical spectral profiles of the two transitions. The class II emission in essentially all the sources consists of one or more narrow ( $< 1 \text{ km s}^{-1}$ ) spectral features. In contrast the class I emission often contains only a single narrow peak, apparently superimposed on broader emission features. Some class I sources do have multiple narrow spectral features, but these are the exception rather than the rule and essentially all sources have the broad emission features rarely seen in the class II emission. Table 1 gives details of the Gaussian profile fitting for each of the class I maser sources and shows that spectral features with widths  $> 1 \text{ km s}^{-1}$  are ubiquitous. It is not clear whether the broad features are quasi-thermal/quasi-maser emission, or perhaps due to blending of a number of weaker maser features. The degree of symmetry and lack of multiple peaks favours the former interpretation. However, interferometric observations are required to provide a definitive answer. The peak flux density and the noise level in the observations of the two classes are comparable and so it cannot be attributed to poorer signal to noise ratio in the class I observations.

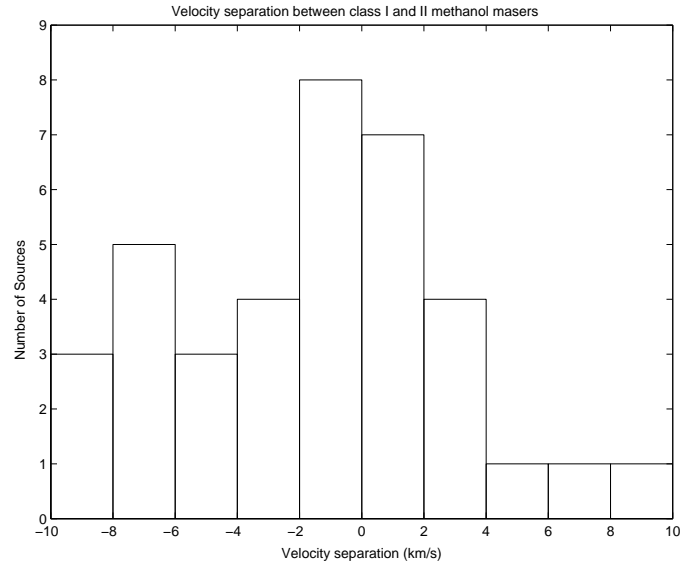


**Figure 3.** The difference between the velocity ranges of the class I 95.1-GHz methanol masers and the corresponding class II 6.6-GHz transition. A negative value indicates that the emission from the two classes overlaps.

Focusing on the statistically complete sample of sixty-six class II methanol masers (those masers not included in this sample are noted in Tables 1 and 3), there are a total of twenty-five detections of associated class I masers. This represents a detection rate of  $38 \pm 6$  per cent for class I methanol masers towards class II sources. However, as the 95.1-GHz transition is not the strongest of the class I transition this figure should be taken as a lower limit. Val'tts et al. (2000) showed that the 44-GHz transition is typically a factor of 3 stronger than the 95.1-GHz transition and so the number of class II methanol masers with an associated class I maser is likely to be of the order of 50 per cent or more.

### 3.1 Comments on individual sources

*326.475+0.703:* The class II methanol maser emission in this source is dominated by two strong peaks separated by more than  $10 \text{ km s}^{-1}$  each of which have a noticeably sharper inner edge than outer edge. The class I maser emission lies in between the two class II peaks, with the red wing of the 95.1-GHz masers overlapping the velocity range of the strongest 6.6-GHz emission. The 6.6-GHz observation spectrum in Fig. 1 is a new observation, however the relative intensity of the two main features appears to have changed little in the 11 years since the discovery of this source (van der Walt, Gaylard & MacLeod 1995)

*326.859-0.667:* The class I and II methanol maser emission in this source each have comparable peak flux density and velocity range, but are offset from each other by approximately  $10 \text{ km s}^{-1}$ , one of the largest offsets in the sample.

*328.237-0.548:* The class II methanol maser emission in this source covers two separate velocity ranges and the class I emission lies in between these. 95.1-GHz class I methanol maser emission was first observed in this source by Val'tts et al. (2000) (who called it 328.24-0.55) and there has been no measurable change in the peak flux density of

**Table 3.** Comparison of the peak flux density and velocity range of 6.6-GHz class II and 95.1-GHz class I methanol masers. Notes : <sup>a</sup> sources not within the statistically complete sample of 6.6-GHz methanol masers. References from which the 6.6- and 95.1-GHz information was obtained : \* = this paper ; 1 = Val'tts et al. (2000) ; 2 = Ellingsen (1996) ; 3 = Ellingsen et al. (1996); 4 = Caswell (1996). For a comprehensive list of references for each 6.6-GHz masers see Pestalozzi et al. (2004).

Source Name	95.1-GHz Class I methanol masers			Ref	6.6-GHz Class II methanol masers			Ref
	Density (Jy)	Velocity (km s <sup>-1</sup> )	Velocity Range (km s <sup>-1</sup> )		Density (Jy)	Velocity (km s <sup>-1</sup> )	Velocity Range (km s <sup>-1</sup> )	
285.32−0.03				1	11	0.6	-8 − 3	2
291.28−0.71				1	70	-29.7	-31 − -26	2
293.84−0.78				1	4	36.9	36 − 39	2
293.95−0.91				1	8	41.4		2
326.475+0.703	29	-41.0	-43 − -38	1	109	-38.1	-51 − -37	*
326.641+0.613 <sup>a</sup>	19	-39.9	-41 − -37	1	17	-43.1	-44 − -40	3
326.662+0.521				1	5	-41.0	-42 − -29	3
326.859−0.677 <sup>a</sup>	11	-67.0	-68 − -66	1	10	-57.6	-59 − -57	3
327.120+0.511				*	80	-87.1	-90 − -83	3
327.392+0.199	8	-89.5	-90 − -88	1	9	-84.6	-86 − -82	3
327.401+0.445				*	106	-82.6	-84 − -75	3
327.402+0.444				*	106	-82.6	-84 − -75	3
327.590−0.094				*,1	3	-86.3		3
327.618−0.111	7	-88.4	-89 − -87	1	2	-97.5		3
327.945−0.115				1	7	-51.7	-52 − -51	3
328.254−0.532					425	-37.4	-50 − -36	3
328.237−0.548 <sup>a</sup>	10	-41.3	-45 − -38	*,1	421	-44.9	-46 − -34	3
328.809+0.633 <sup>a</sup>	45	-40.6	-46 − -37	*,1	278	-44.5	-47 − -43	3
329.031−0.198	20	-43.7	-48 − -39	*	25	-41.9	-47 − -41	3
329.029−0.205	18	-43.6	-47 − -37	1	275	-37.5	-41 − -34	3
329.066−0.308	5.6	-42.1	-43 − -40	*,1	24	-43.9	-48 − -43	3
329.183−0.314	8	-50.1	-51 − -47	1	13	-55.7	-60 − -51	3
329.339+0.148				1	14	-106.5	-107 − -105	3
329.407−0.459				*	144	-66.8	-71 − -66	3
329.469+0.502	9	-66.6	-70 − -66	1	13	-72.1	-73 − -65	3
329.622+0.138				1	30	-60.1	-69 − -59	3
329.610+0.114				1	30	-60.1	-69 − -59	3
330.952−0.182 <sup>a</sup>				*	7	-87.6	-89 − -87	3
331.425+0.264 <sup>a</sup>				1	25	-88.6	-91 − -88	3
331.120−0.118 <sup>a</sup>				1	9	-93.2	-95 − -88	4
331.132−0.244	32	-91.2	-81 − -92	*,1	34	-84.4	-92 − -84	3
331.278−0.188				*	165	-78.1	-86 − -78	3
331.342−0.346	13	-65.7	-67 − -65	*,1	66	-67.4	-68 − -64	3
331.442−0.187 <sup>a</sup>	4.9	-91.7	-92 − -87	*,1	70	-88.5	-93 − -84	3
331.542−0.066				*	12	-84.1	-87 − -83	3
331.556−0.121 <sup>a</sup>				*	35	-103.4	-105 − -94	3
332.094−0.421				1	16	-61.4	-62 − -58	3
332.295−0.094	5.9	-49.7	-50 − -48	*,1	6	-47.0	-47 − -42	3
332.351−0.436				1	4	-53.1		3
332.560−0.148				1	5	-51.0	-56 − -49	3
332.604−0.167	10	-45.7	-47 − -45	1	5	-51.0	-56 − -49	3
332.942−0.686 <sup>a</sup>	9	-48.9	-51 − -47	*	21	-52.9	-54 − -52	3
332.963−0.679 <sup>a</sup>	11	-47.4	-51 − -46	*	41	-45.9	-48 − -38	3
333.029−0.015				*	3	-53.6	-61 − -53	3
333.029−0.063 <sup>a</sup>	4.6	-40.9	-42 − -39	*	4	-40.4	-41 − -40	4
333.068−0.447				*	12	-54.5	-55 − -53	3
333.121−0.434	11	-50.7	-56 − -47	*	11	-49.3	-50 − -48	3
333.128−0.440	46	-48.3	-55 − -45	*,1	3	-44.4	-45 − -42	3
333.130−0.560 <sup>a</sup>	10	-59.0	-61 − -54	*	17	-56.8	-63 − -52	3
333.163−0.101 <sup>a</sup>	4.6	-91.2	-92 − -90	*	8	-95.3	-95 − -91	3
333.184−0.091	7	-87.0	-87 − -85	*	7	-82.0	-85 − -81	3
333.234−0.062	150	-87.4	-91 − -84	*,1	7	-84.7	-85 − -81	3
333.315+0.105	4.2	-44.5	-50 − -43	*	9	-43.7	-50 − -41	3
333.466−0.164	12	-42.8	-46 − -40	*	41	-42.4	-49 − -37	3
333.562−0.025	17	-39.8	-41 − -39	*	39	-35.9	-37 − -34	3
333.646+0.058 <sup>a</sup>				*	3	-87.3	-89 − -82	4
333.683−0.437				*	19	-5.2	-6 − -4	3
333.931−0.135				*	7	-36.8	-37 − -36	3
334.635−0.015				*	61	-30.1	-31 − -27	3

Table 3 – *continued*

Source Name	95.1-GHz Class I methanol masers				6.6-GHz Class II methanol masers			
	Density (Jy)	Peak Flux Velocity (km s <sup>-1</sup> )	Velocity Range (km s <sup>-1</sup> )	Ref	Density (Jy)	Peak Flux Velocity (km s <sup>-1</sup> )	Velocity Range (km s <sup>-1</sup> )	Ref
334.935–0.098 <sup>a</sup>				*	7	-19.5	-22 – -17	4
335.060–0.427 <sup>a</sup>	4.6	-39.1	-41 – -37	*	15	-47.0	-48 – -39	3
25.386+0.005				*	2	95.7	94 – 98	2
25.411+0.105				*,1	8	97.0	96 – 98	2
25.53+0.38				*,1	6	95.6	89 – 96	2
25.710+0.044				*	502	95.7	89 – 101	2
25.826–0.178	58	90.2	90 – 99	*,1	70	91.7	90 – 100	2
26.528–0.266				*	9	104.5	104 – 105	2
26.602–0.220	8	108.1	108 – 114	*	9	103.8	102 – 115	2
27.223+0.137				*	22	117.7	110 – 121	2
27.286+0.151 <sup>a</sup>	4.0	31.7	31 – 34	*	23	34.9	34 – 36	*
27.369–0.164	35	94.2	88 – 96	*	42	100.5	88 – 104	2
28.151–0.002				*	37	101.2	100 – 105	2
28.201–0.049					2	98.9	94 – 99	2
28.303–0.389	4.3	73.9	74 – 75	*	71	81.1	80 – 94	2
28.829+0.488				*	5	83.2	83 – 84	2
28.863–0.237				*	65	83.5	81 – 93	2
28.810+0.360				*	6	91.1	87 – 93	2
29.313–0.165				*	4	48.8	43 – 50	2
29.867–0.042				*	35	101.4	100 – 104	2
29.865–0.007				*	2	103.4	100 – 104	2
29.895–0.047				*	40	96.8	96 – 99	2
29.907–0.040	26	98.2	98 – 99	*	3	99.0	95 – 99	2
29.918–0.035				*	40	96.8	95 – 99	2
29.923+0.059				*	5	99.0	95 – 102	2
29.974–0.029	3.4	96.3	96 – 97	*,1	80	96.0	95 – 100	2
30.009–0.017				*	10	98.3	98 – 103	2

the source in the 12 month period between the two observations.

*328.809+0.633*: This strong class II methanol maser source is associated with a strong class I methanol maser. The peak flux density of the 95.1-GHz methanol masers is more than a factor four greater than observed by Val'tts et al. (2000) a year earlier. The bulk of the class I maser emission is red-shifted compared to the class II emission, but the wing overlaps the velocity of the strongest class II masers.

*329.029–0.205* & *329.031–0.198*: These two class II maser sites are separated by 26 arcsec and each also has associated 95.1-GHz class I methanol maser emission. The spectrum of the 95.1-GHz methanol masers in 329.029–0.205 are blue-shifted with respect to the strongest 6.6-GHz class II emission. The class I methanol maser emission in 329.031–0.198 partially overlaps that of 329.029–0.205, but the peak velocity differs slightly. In contrast to 329.029–0.205, in 329.031–0.198 the velocity ranges of the class I and II methanol masers are largely overlapping.

*329.469+0.502*: This relatively weak, newly discovered 95.1-GHz class I maser source shows weak emission at velocities between the two class II maser velocity ranges in this source.

*331.132–0.244*: The 95.1-GHz class I masers in this source differ from the majority in showing multiple narrow peaks over a substantial velocity range. The velocity of the class I and II methanol masers in this source overlap to a high degree. The strongest class I emission is at the opposite end of the velocity range to the strongest class II masers. However, the 6.6-GHz methanol masers in this sources are known to

be highly variable (Caswell, Vaile & Ellingsen 1995a). The intensity of the entire 95.1-GHz spectrum has increased compared to that observed by Val'tts et al. (2000), suggesting that it is also variable.

*331.342–0.346*: The 95.1-GHz class I maser in this source contains a single narrow peak, lacking the broader velocity feature seen in many sources. The class I maser peak lies in the middle of the class II maser velocity range.

*332.942–0.686* & *332.963–0.679*: The two regions of 6.6-GHz class II methanol maser emission are separated by 1.3 arcmin, but have non-overlapping velocity ranges. Each region also has newly discovered, class I maser emission, the velocity ranges of which overlap, but have distinct peak velocities. The class I emission in each case lies in between the class II velocity ranges of the two sources.

*333.029–0.063*: The new 6.6-GHz Mt Pleasant observations of this source failed to detect any class II methanol maser emission stronger than approximately 2 Jy, so only the 95-GHz spectrum is shown for this source. The observations of Caswell (1996) show that the velocity of the peak of the class I and II methanol masers are separated by 0.5 km s<sup>-1</sup>.

*333.121–0.434* & *333.128–0.440*: There are a number of class II methanol maser sources in this region, two of which also have associated class I maser emission. 333.121–0.434 is a newly discovered 95.1-GHz class I maser source whose velocity range overlaps the class II emission. The 95.1-GHz emission in 333.128–0.440 was also observed by Val'tts et al. (2000), but with a significantly lower peak flux density.

*333.130–0.560*: The 6.6-GHz methanol maser in this source

has an interesting velocity profile consisting of three narrow peaks, the strongest which is bracketed by approximately equal, weaker features. Intriguingly the newly discovered class I 95.1-GHz masers are centred on the same velocity, with symmetrical emission lying within velocity range of the class II methanol masers. This source would be an interesting candidate for high-resolution observations in both transitions to determine the spatial relationship between the two classes.

*333.163–0.101:* The 95.1-GHz methanol maser emission in this source shows two weak peaks separated in velocity by nearly  $20 \text{ km s}^{-1}$ , one of which is close to the velocity of the class II masers. This velocity range is much greater than that seen in any of the other class I methanol masers in this sample, suggesting that perhaps it is a separated source detected within the same beam. This region of the Galactic Plane has been covered in two independent untargeted searches for 6.6-GHz class II masers (Ellingsen et al. 1996; Caswell 1996). If the feature at  $-110 \text{ km s}^{-1}$  is indeed an independent source detected by serendipity it suggests there may be a substantial number of class I maser sources associated neither with class II methanol masers, nor high-mass star formation regions known from other tracers.

*333.234–0.062* With a peak flux density of  $150 \text{ Jy}$  the 95.1-GHz class I methanol maser in this source is the strongest in this sample and is one of the strongest class I masers in this transition. Val’tts et al. (2000) observed a significantly lower peak flux density ( $26 \text{ Jy}$ ) suggesting either a significant pointing offset in their observations, or variability. The class I maser emission is associated with a weak class II methanol maser which has a single peak and non-overlapping velocity range.

*333.315+0.105:* This weak, newly discovered 95.1-GHz methanol maser has a velocity range which overlaps completely with the class II maser emission.

*333.466–0.164:* This newly discovered class I methanol maser source is unusual in that the peak velocity of the class I and II transitions differ by less than  $0.5 \text{ km s}^{-1}$ .

*25.826–0.178:* This site of this strong, newly discovered 95.1-GHz methanol maser was previously searched by Val’tts et al. (2000), but they report no emission stronger than  $3 \text{ Jy}$ . There is a difference in the positions observed in this work and by Val’tts et al. (2000) of  $30 \text{ arcseconds}$ , which is significant, but does not completely account for the non-detection. The class I and II methanol maser emission in this source is notable for having very similar spectra, in terms of peak intensity, velocity range and general shape.

*27.286+0.151:* The velocity of the maser emission in this source lies outside the range of the original Mt Pleasant survey. However, this source was detected in ATCA follow-up observations of  $27.223+0.137$ . It was also independently discovered by Slysh et al. (1999) and Szymczak et al. (2000). The 6.6-GHz spectrum shown in Fig. 1 is a new observation, the earlier observations each show a lower peak flux density, but otherwise similar spectra. The weak, newly detected class I methanol maser in this source doesn’t overlap in velocity with the class II emission.

*28.303–0.389:* The marginal detection of 95.1-GHz methanol maser emission in this source requires follow-up to confirm if it is real. It is offset by more than  $5 \text{ km s}^{-1}$  from the class II emission, which is unusual, but the class II emission does extend over a larger than usual range in this source.

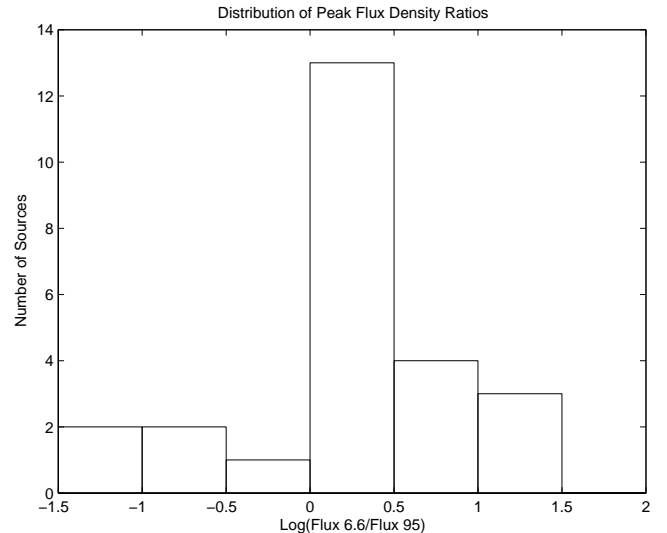


**Figure 4.** Comparison of the distribution of ratio of the 6.6-GHz peak flux density to the associated 95-GHz peak flux density for the twenty-five methanol masers in the statistically complete sample.

*29.907–0.040:* There are five additional class II methanol maser sites within a relatively small distance of this source and they have overlapping velocity ranges. A 95.1-GHz class I methanol maser was detected towards a number of the class II sites. However, it appears to be a single source which is strongest at this location. Disentangling the relationship of the different star-formation sites within this complex will require interferometric observations.

*29.974–0.029:* The marginal detection of 95.1-GHz methanol maser emission in this source requires a follow-up to confirm if it is real. Emission of comparable strength at the same velocity was detected by Val’tts et al. (2000) and so this emission is likely to be real.

## 4 DISCUSSION

Slysh et al. (1994) claim that there is an anti correlation between the flux density of class I and class II methanol masers within the same region. It is certainly true that the strongest class II masers typically do not have associated class I masers (e.g. W3(OH), NGC6334F) and vice versa. This was one of the factors in the empirical classes as they were originally defined. However, the current observations show that for typical methanol masers there is no anti-correlation between the peak flux density of the class I and II maser transitions. Considering the twenty-five masers within the statistically complete sample that have an associated class I maser, the 6.6- and 95.1-GHz peak flux densities are in general comparable with a median ratio of 1.25. Figure 4 shows that the distribution of peak flux density ratios is strongly peaked at values slightly greater than one.

There are significant differences between the typical morphologies observed for class I and class II methanol masers. Class II methanol maser emission occurs in clusters with a maximum size of  $30 \text{ milli-parsecs}$  Caswell (1997); Phillips et al. (1998). The majority of sources have just one

cluster, some have a second cluster separated by a few arcseconds, but more than two separate clusters in one region is very rare. In contrast the emission from class I masers is typically spread over much larger angular scales Kogan & Slysh (1998); Kurtz et al. (2004). This suggests enhanced methanol abundance over a significant fraction of the star formation region, but that conditions suitable for class II masers are relatively rare, while those that favour class I masers are more common.

Early interferometric observations of class I methanol masers suggested that they may be associated with outflows from high-mass star formation regions, perhaps at the interface between the outflow and the molecular cloud (Plambeck & Menten 1990; Johnston et al. 1992). That they are observed offset from HII regions, and are collisionally pumped is also consistent with this hypothesis. Further support has recently been provided by the observations of Kurtz et al. (2004) who found a number of sources for which there is a good correspondence between the 44 GHz class I masers and the molecular shock tracers  $H_2$  and SiO.

It is well established that many water masers in star formation regions are associated with outflows, some of which have velocities in excess of 100 km/s and are highly collimated. Interferometric observations of water masers have shown that those with the largest peak flux densities lie in outflows directed at angles close to the plane of the sky (Genzel et al. 1981a,b). With this geometry our line-of-sight looks along the shock-front, giving a long velocity coherent path and hence strong masers. In contrast, masers which are significantly offset from the systemic velocity of the system are in outflows directed close to the line-of-sight, we view the shock-fronts close to face on resulting in short gain paths and weak masers.

The class I methanol masers are clearly not associated with the same outflows (or at least with the same parts of the outflows), as water masers, as they are always within  $10\text{--}20\text{ km s}^{-1}$  of the velocity of class II masers and thermal emissions. However, we might expect class I methanol masers which are close to the systemic velocity of the region to be associated with outflows directed close to the plane of the sky and, analogous to water masers to be stronger. If we assume that the velocity of the class II masers is close to the systemic velocity of the region (which is generally the case), then we can test this hypothesis by comparing the flux density of class I masers which overlap the velocity range of the class II with those that don't. Figure 5 shows two histograms which make this comparison. Only those class I methanol masers associated with class II masers in the statistically complete sample are included in Fig. 5. The two samples (18 sources which have overlap and 7 sources which don't) are too small to allow definitive conclusions to be drawn. However, there may be a higher percentage of stronger class I methanol masers associated with sources where there is a velocity overlap between the two classes.

Two types of observations suggest that class II methanol masers are associated with the early stages of high-mass star formation.

- (i) Many class II methanol masers are not associated with an UCHII region (Phillips et al. 1998; Walsh et al. 1998).
- (ii) Class II masers are associated with submillimetre and millimetre dust continuum emission which have SED con-

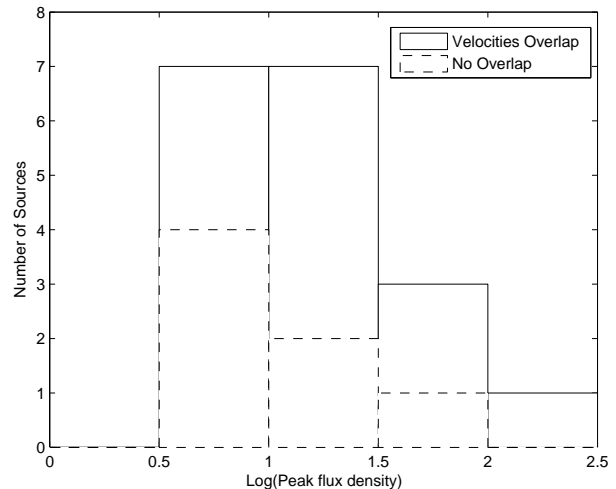


**Figure 5.** Comparison of the distribution of peak flux density for class I methanol masers which have a velocity range which overlaps the class II masers (solid line) and those which do not (dashed line). Only class I masers associated with class II masers in the statistically complete sample are included in this figure.

sistent with deeply embedded high-mass protostellar objects Pestalozzi, Humphreys & Booth (2002); Walsh et al. (2003); Minier et al. (2004)

The current star formation paradigm for low-mass star formation has molecular outflows associated with the earliest stages of the process, the so-called class 0 and class I young stellar objects (Bachiller & Tafalla 1999). From this we might hypothesise that class I methanol masers may be associated with an even earlier stage of high-mass star formation than is the general case for class II masers. Considering only methanol masers we might expect sources with only class I methanol masers to be the youngest, with those which have both class I and II masers being at an intermediate phase and sources with only class II methanol masers being the most evolved. We can test this hypothesis by looking at the properties of the infrared sources and other maser species associated with the methanol masers and seeing if there is any difference between the class II masers with and without an associated class I maser. If a difference can be found then it would also provide a method of targeting class I methanol maser searches.

The two most common masers associated with high-mass star formation (apart from class II methanol masers) are the 1665-MHz transition of OH and the 22-GHz transition of water. An untargted search of the southern Galactic plane for main-line OH masers was made with the Parkes telescope in the early 1980s (Caswell et al. 1980; Caswell & Haynes 1983a, 1987), with some regions more recently searched again at higher sensitivity with the Australia Telescope Compact Array (Caswell 1998). The Parkes search was sensitive to OH masers with a peak flux density in excess of 1 Jy in the main-line transition at the epoch of the observations. To date there have been no blind searches for southern water masers. However, a search targeted towards the 6.6-GHz methanol masers detected in the Mt Pleasant survey has been undertaken by Hanslow (1997). Table 4 sum-

marises the association of the class II methanol masers from the Mt Pleasant survey with 1665-MHz OH and 22-GHz water masers. Considering only the class II methanol masers in the statistically complete sample, approximately 30 percent have an associated 1665-MHz OH maser and approximately 40 percent have an associated water maser. However, there is no statistically significant correlation, or anti-correlation between the presence of OH or water masers and class I methanol masers.

#### 4.1 Infrared characteristics of class I and II methanol masers

A number of searches for class II methanol masers have been targeted towards *IRAS* sources with far-infrared colours within certain ranges (e.g. Schutte et al. 1993; Walsh et al. 1997; Slysh et al. 1999; Szymczak et al. 2000). The current class I maser observations were targeted towards class II methanol maser positions, the vast majority of which are known to sub-arcsecond accuracy. So it is possible to reliably determine whether infrared sources from the *IRAS*, *MSX* and 2MASS point sources catalogues are associated with the maser positions. If the sources with class I methanol masers represent a different evolutionary phase from those without then this may lead to an observable difference in the properties of associated infrared sources. In this section we examine the characteristics of *IRAS*, *MSX* and 2MASS sources associated with the masers to see if there is any difference between those class II methanol masers with and without associated class I masers. Some readers may prefer to skip to the concluding paragraph of this section where the results are summarised, rather read all the details of the comparisons undertaken that are given below.

Considering only the statistically complete sample of sixty-eight class II methanol masers, 30 have an associated *IRAS* point source (IRAS Science Working Group 1985) within 30 arcsec, 45 have an associated *MSX* point source (Egan et al. 2003) within 30 arcsec and 45 have an associated 2MASS source within 5 arcsec. The names and the distance between the infrared point source and maser positions are summarised in table 5.

There are 11 *IRAS* sources which exhibit both class I and II methanol maser emission (version 2.1 of the *IRAS* PSC). This is consistent with the number expected by chance considering the relative proportions of class II methanol maser sources with associated class I masers and *IRAS* sources. Examining a plot of the  $F_{25}/F_{12}$  versus  $F_{60}/F_{25}$  colours (where  $F_{12}$ ,  $F_{25}$  and  $F_{60}$  are the *IRAS* 12-, 25- and 60- $\mu$ m flux densities respectively) there is no apparent difference between those *IRAS* sources with and without an associated class I methanol maser. So there doesn't appear to be any means of using *IRAS* colours to select high-mass star forming regions that are more likely to have associated class I methanol masers, beyond the well known ultra-compact HII region criteria developed by Wood & Churchwell (1989). This implies that any evolutionary difference between class II maser sources with and without associated class I masers cannot be distinguished from *IRAS* data.

The *IRAS* observations suffered well documented problems with confusion and saturation close to the Galactic Plane and this is thought to be the reason why many class II

**Table 4.** Associations of the class II methanol masers with other maser species and *MSX* 21- $\mu$ m flux. The *MSX* flux is measured directly from the images, for non-detections the flux density at the maser location is given as an upper limit. Notes : <sup>a</sup> sources not within the statistically complete sample of 6.6-GHz methanol masers. References 1 = Caswell & Haynes (1987) ; 2 = Caswell (1998) ; 3 = Caswell & Haynes (1983b) ; 4 = Caswell et al. (1995b) ; 5 = Hanslow (1997)

Source Name	1665-MHz OH maser Assoc	Ref	22-GHz H <sub>2</sub> O maser Assoc	Ref	MSX 21- $\mu$ m flux ( $\mu$ Wm <sup>-2</sup> sr <sup>-1</sup> )
285.32-0.03	N	1	Y	5	<1.25
291.28-0.71	N	1	Y	5	1600
293.84-0.78	N	1	Y	5	<0.15
293.95-0.91	N	1	Y	5	<0.77
326.475+0.703	N	2	Y	5	<0.87
326.641+0.613 <sup>a</sup>	N	2	Y	5	<12.5
326.662+0.521	N	2	Y	5	330
326.859-0.677 <sup>a</sup>	N	2	N	5	<3.6
327.120+0.511	Y	2	Y	5	71
327.392+0.199	N	2	N	5	9.6
327.401+0.445	N	2	N	5	55
327.402+0.444	Y	2	Y	5	41
327.590-0.094	N	2	N	5	9.5
327.618-0.111	N	2	N	5	8.1
327.945-0.115	N	2	N	5	57
328.254-0.532	Y	2	Y	5	53
328.237-0.548 <sup>a</sup>	Y	2	Y	5	7.6
328.809+0.633 <sup>a</sup>	Y	2	N	5	510
329.031-0.198	Y	2	Y	5	<4.0
329.029-0.205	Y	2	Y	5	<3.6
329.066-0.308	Y	2	N	5	20
329.183-0.314	Y	2	Y	5	<5.7
329.339+0.148	N	2	N	5	700
329.407-0.459	Y	2	Y	5	19
329.469+0.502	N	2	N	5	<4.7
329.622+0.138	N	2	Y	5	<0.53
329.610+0.114	N	2	N	5	27
330.952-0.182 <sup>a</sup>	Y	2	Y	5	130
331.425+0.264 <sup>a</sup>	N	2	N	5	<3.8
331.120-0.118 <sup>a</sup>	N	2	Y	5	<3.1
331.132-0.244	Y	2	Y	5	21
331.278-0.188	Y	2	Y	5	95
331.342-0.346	Y	2	N	5	60
331.442-0.187 <sup>a</sup>	Y	2	Y	5	8.7
331.542-0.066	Y	2	N	5	320
331.556-0.121 <sup>a</sup>	Y	2	Y	5	106
332.094-0.421	N	2	Y	5	480
332.295-0.094	N	2	Y	5	71
332.351-0.436	N	2	N	5	<2.8
332.560-0.148	N	2	N	5	<11
332.604-0.167	N	2	N	5	<3.0
332.942-0.686 <sup>a</sup>	N	2	Y	5	<8.6
332.963-0.679 <sup>a</sup>	N	2	N	5	31
333.029-0.015	N	2	N	5	<4.8
333.029-0.063 <sup>a</sup>	N	2		5	32
333.068-0.447	N	2	N	5	120
333.121-0.434	N	2	Y	5	420
333.128-0.440	N	2	Y	5	420
333.130-0.560 <sup>a</sup>	N	2	Y	5	<7.1
333.163-0.101 <sup>a</sup>	N	2	N	5	58
333.184-0.091	N	2	N	5	<11
333.234-0.062	Y	2	Y	5	<6.0
333.315+0.105	Y	2	N	5	56
333.466-0.164	Y	2	Y	5	29
333.562-0.025	N	2	N	5	<3.9



**Table 5.** Associations of the class II methanol masers with *IRAS*, *MSX* and 2MASS point sources. Notes : <sup>a</sup> sources not within the statistically complete sample of 6.6-GHz methanol masers.

Source Name	IRAS Name	IRAS Distance (arcsec)	MSX Name	MSX Distance (arcsec)	2MASS Name	2MASS Distance (arcsec)
285.32−0.03	10303−5746	21.4	G285.3472+00.0013	17.9	10321294−5802306	4.8
291.28−0.71	11097−6102	19.4	G291.2731−00.7101	16.0	11115460−6118279	2.7
293.84−0.78	11298−6155	1.3	G293.8282−00.7445	1.6	11320631−6212206	2.4
293.95−0.91	11304−6206	1.1	G293.9512−00.8941	6.4	11324316−6223048	2.2
326.475+0.703	15394−5358	20.8			15431671−5407089	3.8
326.641+0.613 <sup>a</sup>					15443293−5405293	0.8
326.662+0.521	15412−5359	6.9	G326.6618+00.5207	0.8	15450281−5409030	0.4
326.859−0.677 <sup>a</sup>						
327.120+0.511	15437−5343	3.6	G327.1192+00.5103	1.9	15473282−5352398	1.2
327.392+0.199	15464−5348	4.0	G327.3941+00.1970	12.2	15501855−5357087	2.4
327.401+0.445			G327.4014+00.4454	3.4		
327.402+0.444			G327.4014+00.4454	4.5	15491950−5345096	4.5
327.590−0.094					15523652−5403157	4.1
327.618−0.111			G327.6184−00.1109	0.4	15525032−5402596	1.3
327.945−0.115	15507−5341	2.8	G327.9455−00.1149	3.5	15543391−5350446	0.1
328.254−0.532	15541−5349	2.7	G328.2523−00.5320	5.9		
328.237−0.548 <sup>a</sup>			G328.2396−00.5460	12.3		
328.809+0.633 <sup>a</sup>	15520−5234	4.1	G328.8074+00.6324	4.7	15554848−5243018	4.5
329.031−0.198	15566−5304	8.4			16003085−5312268	4.8
329.029−0.205	15566−5304	17.6				
329.066−0.308	15573−5307	2.2	G329.0663−00.3081	2.2	16010999−5316029	0.6
329.183−0.314	15579−5303	5.2				
329.339+0.148	15567−5236	5.9	G329.3371+00.1469	7.7		
329.407−0.459	15596−5301	13.1	G329.4055−00.4574	8.1		
329.469+0.502			G329.4626+00.5037	23.2	15594047−5223265	2.6
329.622+0.138					16020013−5233578	2.0
329.610+0.114			G329.6098+00.1139	1.2	16020313−5235328	0.7
330.952−0.182 <sup>a</sup>			G330.9544−00.1817	6.8	16095195−5154595	4.2
331.425+0.264 <sup>a</sup>						
331.120−0.118 <sup>a</sup>			G331.1195−00.1191	4.5		
331.132−0.244	16071−5142	26.7	G331.1282−00.2436	12.8	16105979−5150253	2.7
331.278−0.188	16076−5134	10.4	G331.2759−00.1891	8.7		
331.342−0.346			G331.3402−00.3444	8.5	16122648−5146177	0.9
331.442−0.187 <sup>a</sup>			G331.4442−00.1877	9.0		
331.542−0.066			G331.5414−00.0675	5.1	16120865−5125488	3.6
331.556−0.121 <sup>a</sup>	16086−5119	26.6	G331.5582−00.1206	9.5	16122682−5127389	3.7
332.094−0.421	16124−5110	3.8	G332.0939−00.4206	1.3	16161646−5118251	0.3
332.295−0.094	16119−5048	8.1	G332.2944−00.0962	9.7	16154514−5055511	3.4
332.351−0.436	16137−5100	9.6			16173117−5108181	5.0
332.560−0.148			G332.5555−00.1429	23.5		
332.604−0.167						
332.942−0.686 <sup>a</sup>	16175−5046	23.0	G332.9419−00.6849	3.3		
332.963−0.679 <sup>a</sup>	16175−5045	2.8	G332.9636−00.6800	4.3		
333.029−0.015			G333.0274−00.0131	9.3	16184404−5021487	2.4
333.029−0.063 <sup>a</sup>			G333.0299−00.0645	7.1	16185660−5023542	1.2
333.068−0.447			G333.0682−00.4461	3.3		
333.121−0.434			G333.1256−00.4367	20.2	16205937−5035516	3.2
333.128−0.440			G333.1256−00.4367	14.6	16210349−5035505	2.0
333.130−0.560 <sup>a</sup>					16213571−5040527	1.5
333.163−0.101 <sup>a</sup>	16159−5012	20.3	G333.1642−00.0994	5.6	16194245−5019532	2.0
333.184−0.091					16194611−5018365	5.0
333.234−0.062					16195102−5015176	4.1
333.315+0.105	16157−4957	2.9	G333.3151+00.1053	0.8	16192910−5004432	2.0
333.466−0.164	16175−5002	12.7	G333.4680−00.1603	16.1		
333.562−0.025					16210884−4959484	0.5
333.646+0.058 <sup>a</sup>			G333.6506+00.0598	20.2	16210963−4952455	4.8
333.683−0.437	16196−5005	14.0	G333.6788−00.4344	15.5	16232951−5012118	4.1
333.931−0.135	16194−4941	25.0	G333.9305−00.1319	9.4		
334.635−0.015	16220−4906	7.9	G334.6340−00.0125	8.6	16254596−4913388	2.6
334.935−0.098 <sup>a</sup>					16272411−4904076	3.9
335.060−0.427 <sup>a</sup>	16256−4905	17.6	G335.0611−00.4261	7.6	16292288−4912259	3.0

Table 5 – *continued*

Source Name	IRAS Name	Distance (arcsec)	MSX Name	Distance (arcsec)	2MASS Name	Distance (arcsec)
25.386+0.005			G025.3865+00.0036	6.8		
25.411+0.105	18345–0641	4.6	G025.4118+00.1052	3.0	18371690–0638304	2.2
25.53+0.38					18363259–0624251	0.9
25.710+0.044			G025.7058+00.0403	19.1		
25.826–0.178					18390338–0624096	3.6
26.528–0.266			G026.5254–00.2667	9.6		
26.602–0.220						
27.223+0.137			G027.2220+00.1361	5.3	18403043–0500569	1.9
27.286+0.151 <sup>a</sup>					18403448–0457137	0.3
27.369–0.164	18391–0504	12.5	G027.3652–00.1638	12.1		
28.151–0.002			G028.1467–00.0040	15.9		
28.201–0.049	18403–0417	3.9	G028.2007–00.0494	0.7	18425811–0413573	1.4
28.303–0.389			G028.3046–00.3871	10.0	18442217–0417463	3.0
28.829+0.488					18421219–0325376	4.1
28.863–0.237						
28.810+0.360						
29.313–0.165	18427–0320	29.5			18452474–0317411	4.8
29.867–0.042			G029.8620–00.0444	20.7	18455964–0244453	2.6
29.865–0.007						
29.895–0.047					18460337–0243223	4.9
29.907–0.040					18460346–0242394	3.6
29.918–0.035			G029.9183–00.0404	19.8		
29.923+0.059					18454403–0239052	2.7
29.974–0.029			G029.9738–00.0364	28.2	18460869–0238420	2.9
30.009–0.017						

methanol maser sites have no associated *IRAS* source. Since if all class II methanol masers are associated with high-mass star formation (as argued the introduction) then they should show far-infrared emission, even those that are very young and enshrouded in cold dust. The *MSX* and 2MASS observations do not have the same problems as *IRAS*. However, they were made at shorter, mid- and near-infrared wavelengths. A total of 45 of the class II methanol maser sources in the statistically complete sample have an associated *MSX* source within 30 arcsec, and of these 14 also have an associated class I methanol maser. Version 2.3 of the *MSX* point source catalogue was used, which contains more than 25 percent more sources, and has greater photometric accuracy than earlier versions of the catalogue (Egan et al. 2003). If the sources with class I masers represent an earlier evolutionary phase then we would expect them to be more deeply embedded, and likely to show a lower rate of detection in the mid-infrared *MSX* observations. However, the proportion of class I methanol maser sources with an associated *MSX* source is within the range expected given the rate of association with the parent sample. Lumsden et al. (2002) investigated the *MSX* colours of a sample of massive young stellar objects (MYSO) and found that they show  $F_8 < F_{12} < F_{21}$  (where  $F_8$ ,  $F_{12}$  and  $F_{21}$  are the *MSX* 8-, 12- and 21- $\mu$ m flux densities respectively) and  $F_{21}/F_8 > 2$ . Figure 6 shows an *MSX* colour-colour plot of  $F_{14}/F_{12}$  versus  $F_{21}/F_8$  for the class II methanol maser sources with and without associated class I methanol masers, and included for comparison are all *MSX* sources within 30 arcsec of  $l = 326^\circ$ ,  $b = 0^\circ$ . The majority of the maser sources meet the Lumsden et al. (2002) criteria for MYSO, that is

they lie within the top right section of Fig 6. This is not particularly surprising as 6.6-GHz methanol masers without associated radio continuum emission from Walsh et al. (1998) were part of the sample of sources used to define the criteria. However, that a statistically complete sample of class II methanol masers shows the same characteristics in an *MSX* colour-colour plot as the *IRAS*-selected sample of Walsh et al. adds further weight to the widely accepted argument that the new class II methanol masers discovered in untargeted searches are in fact associated with high-mass star formation. The further towards the top-right of Fig 6 a source lies, the cooler the implied dust temperature, so we would expect younger, more deeply embedded sources to lie in this region. The class II methanol masers with and without associated class I masers show the same distribution, again suggesting that there is no significant evolutionary difference between the two groups.

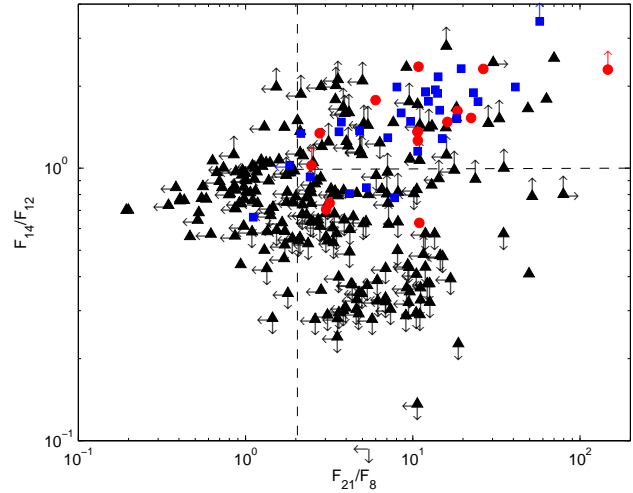
The quoted astrometric accuracy of the *MSX* point source catalogue is better than 2 arcsec (Egan et al. 2003). However, only 8 of the 45 *MSX* sources are within 2 arcsec of the class II maser position. In total 14 of the class II maser positions are within 5 arcsec and 29 are within 10 arcsec of an *MSX* point source. This suggests that in general the masers are offset from the *MSX* point sources, and probably associated with other objects within the larger star formation complex. It suggests that in many cases the colours of the *MSX* sources in Fig. 6 are not those of the source exciting the methanol masers and so will confuse any attempt to find differences between the class II masers with and without associated class I masers. However, it still may be possible to find such differences directly from the *MSX*

Table 4 – continued

Source Name	1665-MHz OH maser		22-GHz H <sub>2</sub> O maser		MSX 21- $\mu$ m flux ( $\mu$ Wm <sup>-2</sup> sr <sup>-1</sup> )
	Assoc	Ref	Assoc	Ref	
333.646+0.058 <sup>a</sup>	N	2		5	<3.3
333.683-0.437	N	2	N	5	1.3
333.931-0.135	N	2	N	5	10.0
334.635-0.015	N	2	N	5	<1.9
334.935-0.098 <sup>a</sup>	N	2		5	<1.4
335.060-0.427 <sup>a</sup>	Y	2	Y	5	17
25.386+0.005	N	3	N	5	<4.4
25.411+0.105	N	3	N	5	28
25.53+0.38	N	3	N	5	<1.7
25.710+0.044	N	3	N	5	21
25.826-0.178	N	3	Y	5	<2.8
26.528-0.266	N	3	N	5	<7.4
26.602-0.220	N	3	N	5	<3.7
27.223+0.137	N	3	N	5	<7.4
27.286+0.151 <sup>a</sup>	N	3	N	5	9.3
27.369-0.164	Y	3	Y	5	11
28.151-0.002	N	3	N	5	<5.2
28.201-0.049	Y	3	N	5	230
28.303-0.389	N	3	N	5	120
28.829+0.488	N	3	Y	5	<1.8
28.863-0.237	Y	3	N	5	<3.6
28.810+0.360	N	3	Y	5	<1.7
29.313-0.165	N	3	N	5	<1.9
29.867-0.042	Y	4	N	5	13
29.865-0.007	N	3	N	5	<2.5
29.895-0.047	N	3	N	5	<11
29.907-0.040	N	3	N	5	14
29.918-0.035	Y	4	N	5	18
29.923+0.059	N	3	N	5	<0.35
29.974-0.029	N	3	Y	5	17
30.009-0.017	N	3	N	5	<4.7

image data. I have examined the 21- $\mu$ m *MSX* (E-band) images in the vicinity of each of the maser sources and the results are summarised in Table 4. If the class I masers are associated with a generally earlier evolutionary phase, then we would expect a lower percentage to be projected against 21- $\mu$ m emission. Considering the sixty-eight class II masers in the complete sample, thirty-five are projected against 21- $\mu$ m emission, 15 of 26 with class I masers and 21 of 42 without. So approximately 50 percent of class II methanol maser sources are projected against 21- $\mu$ m *MSX* emission, but there is no correlation with the presence or absence of associated class I masers. Of those maser sources that are not projected against 21- $\mu$ m emission, some are near a source, but the majority are not. In contrast, for an *IRAS*-selected sample of nearly 50 UCHII regions, only one did not have coincident 21- $\mu$ m *MSX* emission (Crowther & Conti 2003).

Near-infrared observations of methanol maser sources are generally of limited use as most sources are thought to be optically thick at these wavelengths. However, for completeness the association of the methanol masers with sources in the 2MASS point source catalogue has been examined. Considering the statistically complete sample of sixty-eight sources, forty-five have a 2MASS point source within 5 arcsec, dropping to 13 within 2 arcsec. The proportion of these sources which also have an associated class I methanol maser matches the proportions for the sample as a whole. As for the *MSX* sources, it is likely that in many cases the 2MASS



**Figure 6.** *MSX* colours  $F_{14}/F_{12}$  versus  $F_{21}/F_8$  for class II methanol masers with (circles) and without (squares) associated class I masers. The triangles are *MSX* sources within 30 arcsec of  $l = 326^\circ$ ,  $b = 0^\circ$ . Sources with an upper limit in one of the *MSX* bands making up the ratio are marked with an arrow pointing in the appropriate direction. Sources with an upper limit in both *MSX* bands for either of the colours have been excluded from the plot. Sources within region within the dashed lines at the top right of the plot meet the MYSO criteria of Lumsden et al. (2002).

point sources are not directly associated with the masers, but rather a nearby source within the same region.

The association of the class II methanol masers in the statistically complete sample with *IRAS*, *MSX* and 2MASS sources has been investigated. There is no measurable difference, either in terms of rates of association, or the infrared colours between those class II masers with an associated class I maser and those without. Combining this with the similar finding for the association of other maser species, it suggests that class I methanol masers, like class II, are associated with star formation regions for a moderately long evolutionary period. For example 329.031-0.198 is optically thick at a wavelength of 21- $\mu$ m, suggesting it is deeply embedded and at an early evolutionary phase. In contrast 328.809+0.633 has a well developed HII region with some extended emission (Ellingsen, Shabala & Kurtz 2005) and shows emission in a number of the rarer excited OH and class II maser transitions (Ellingsen et al. 2004, and references therein), which are believed to be associated with more evolved regions. The lack of any distinguishing characteristics between the class II masers with and without associated class I masers is consistent with the general assumption that the two classes of methanol maser are not directly associated. High-mass stars form in clusters and so it is likely that at any one time there are stars at a variety of evolutionary phases within the one region. If in general the star exciting the class II methanol masers is not the source of the out-flow producing the class I masers then we would not expect any clear evolutionary relationship to be manifest. However, there are many other possible complicating factors, for example there is no reason to expect both classes of methanol maser to be associated with exactly the same stellar mass range. This complexity further highlights the general need

for high-resolution observations to disentangle a high-mass star formation complex.

## 5 CONCLUSIONS

Class I methanol masers are associated with approximately half of all class II methanol maser sources. In contrast to previous suggestions, there is no anti-correlation between the velocity range of the two maser classes, nor their peak flux densities. The velocity ranges overlap in the majority of sources and there is some evidence that in those sources where there is an overlap the peak flux density of the class I masers is stronger. The peak flux density of the 6.6- and 95.1-GHz transitions in most sources is of the same order of magnitude. This suggests that the peak maser flux density in both transitions may be heavily influenced by a common factor, such as the general methanol abundance within the larger star formation region.

Interferometric observations of the class I masers are required to allow a more detailed examination of the relationship between the two methanol maser classes and their role in the larger high-mass star formation picture. In particular to determine if the overlap in the velocity ranges seen in many sources is associated with coincident or near-coincident emission from the two transitions, or is merely an artefact of turbulent velocity fields.

Investigation of other maser species and infrared sources associated with the methanol masers did not find any statistically significant correlations that can be used to target future class I maser searches. The absence of such correlations is consistent with the hypothesis that the objects responsible for producing class I methanol masers are in general not those that produce main-line OH, water or class II methanol masers, although there are other possible explanations.

## ACKNOWLEDGEMENTS

Thanks to Robina Otrupcek for her assistance with observations. Thanks to Jim Caswell for valuable comments and discussions. Financial support for this work was provided by the Australian Research Council. This research has made use of NASA's Astrophysics Data System Abstract Service and data products from the *Midcourse Space Experiment*. Processing of the data was funded by the Ballistic Missile Defence Organization with additional support from the NASA Office of Space Science. The research has made use of the NASA/IPAC Infrared Science Archive, which is operated by the Jet Propulsion Laboratory, California Institute of Technology, under contract with the National Aeronautics and Space Administration.

## REFERENCES

- Bachiller R., Tafalla M., 1999, in NATO Science series C540, *The Origin of Stars and Planetary Systems*, ed. C. J. Lada & N. D. Kylafis, 227
- Batrla W., Menten K. M., 1988, *ApJ*, 329, 117
- Batrla W., Matthews H. E., Menten K. M., Walmsley C. M., 1987, *Nat*, 326, 49
- Caswell J. L., 1996, *MNRAS*, 279, 79
- Caswell J. L., 1997, *MNRAS*, 289, 203
- Caswell J. L., 1998, *MNRAS*, 297, 215
- Caswell J. L., Haynes R. F., 1983a, *Aust. J Phys.*, 36, 361
- Caswell J. L., Haynes R. F., 1983b, *Aust. J Phys.*, 36, 417
- Caswell J. L., Haynes R. F., Goss W. M., 1980, *Aust. J Phys.*, 33, 639
- Caswell J. L., Haynes R. F., 1987, *Aust. J Phys.*, 40, 215
- Caswell J. L., Vaile R. A., Ellingsen S. P., 1995, *PASA*, 12, 37
- Caswell J. L., Vaile R. A., Ellingsen S. P., Whiteoak J. B., Norris R. P., 1995, *MNRAS*, 272, 96
- Cragg D. M., Johns K. P., Godfrey P. D., Brown R. D., 1992, *MNRAS*, 259, 203
- Crowther P. A., Conti P. S., 2003, *MNRAS*, 343, 143
- De Lucia F. C., Herbst E., Anderson T., Helminger, P., 1989, *J. Mol. Spectrosc.*, 134, 395
- Egan M. P., Price S. D., Kraemer K. E., Mizuno D. R., Carey S. J., Wright C. O., Engelke C.W., Cohen M., Gugliotti G. M., 2003, *The Midcourse Space Experiment Point Source Catalog Version 2.3 Explanatory Guide (AFRL-VS-TR-2003-1589)*. Natl. Tech. Inf. Serv, Springfield, VA.
- Ellingsen S. P., 1996, PhD thesis, University of Tasmania
- Ellingsen S. P., von Bibra M. L., McCulloch P. M., Norris R. P., Deshpande A. A., Phillips C. J., 1996, *MNRAS*, 280, 378
- Ellingsen S. P., Cragg D. M., Lovell J. E. J., Sobolev A. M., Ramsdale P. D., Godfrey P. D., 2004, *MNRAS*, 354, 401
- Ellingsen S. P., Shabala S. S., Kurtz S. E., 2005, *MNRAS*, in press
- Genzel R., Reid M. J., Moran J. M., Downes D., 1981, *ApJ*, 244, 884
- Genzel R., Downes D., Schneps M. H., Reid M. J., Moran J. M., Kogan L. R., Kostenko V. I., Matveenko L. I., Ronnang B., 1981, *ApJ* 247, 1039
- IRAS Point Source Catalog, 1985, IRAS Science Working Group, U.S. Government Printing Office, Washington DC
- Hanslow L. A., 1997, Honours thesis, University of Tasmania
- Houghton S., Whiteoak J. B., 1995, *MNRAS*, 273, 1033
- Johnston K. J., Gaume R., Stolovy, S., Wilson T. L., Walmsley C. M., Menten K. M., 1992, *ApJ*, 385, 232
- Kogan L., Slysh V., 1998, *ApJ*, 497, 800
- Kurtz S., Hofner P., Álvarez C. V., 2004, *ApJSS*, 155, 149
- Kutner M. L., Ulich B. L., 1981, *ApJ*, 250, 341
- Ladd N., Phillips C., Purcell C., Kesteven M., 2004, CSIRO Memo "Specification of Frequency and Velocity Scales for Mopra Spectra"
- Lumsden S. L., Hoare M. G., Oudmaijer R. D., Richards D., 2002, *MNRAS*, 336, 621
- Mehring D. M., Menten K. M., 1997, *ApJ*, 474, 346
- Menten K. M., 1991a, in ASP Conf. Ser. 16, *Atoms, ions and molecules: New results in spectral line astrophysics*, ed. A. D. Haschick & P. T. P. Ho, 119
- Menten K. M., 1991b, *ApJ*, 380, L75
- Minier V., Burton M. G., Hill T., Pestalozzi M. R., Purcell C., Garay G., Walsh A., Longmore S., 2004, *A&A*, in press
- Morimoto M., Ohishi M., Kanzawa T., 1985, *ApJ*, 288, L11
- Müller H. S. P., Menten K. M., Mäder H., 2004, *A&A*, 428, 1019
- Peng R. S., Whiteoak J. B., 1992, *MNRAS*, 254, 301

- Pestalozzi M., Humphreys E. M. L., Booth R. S., 2002, A&A, 384, L15
- Pestalozzi M., Minier V., Booth R., 2004, A&A, in press
- Phillips C. J., Norris R. P., Ellingsen S. P., McCulloch P. M., 1998, MNRAS, 300, 1131
- Plambeck R. L., Menten K. M., 1990, ApJ, 364, 555
- Plambeck R. L., Wright M. C. H., 1988, ApJ, 330, L61
- Schutte A. J., van der Walt D. J., Gaylard M. J., MacLeod G. C., 1993, 261, 783
- Szymczak M., Hrynek G., Kus A. J., 2000, A&AS, 143, 269
- Szymczak M., Kus A. J., Hrynek G., Kepa, A., Pazderski, E., 2002, A&A, 392, 277
- Slysh V. I., Kalenskii S. V., Val'tts I. E., Otrupcek R., 1994, MNRAS, 268, 464
- Slysh V. I., Val'tts I. E., Kalenskii S. V., Voronkov M. A., Palagi F., Tofani G., Catarzi M., 1999, A&AS, 134, 115
- Sobolev A.M., Deguchi S., 1994, A&A, 291, 569
- Sobolev A. M., Cragg D. M., Godfrey P. D., 1997, MNRAS, 288, L39
- Val'tts, I. E., Ellingsen, S. P., Slysh, V. I., Kalenskii, S. V., Otrupcek R., Larinov G. M., 2000, MNRAS, 317, 315
- van der Walt D. J., Gaylard M. J., MacLeod G. C., 1995, A&ASS, 110, 81
- Voronkov M. A., Sobolev A. M., Ellingsen S. P., Ostrovskii A. B., 2004, MNRAS submitted
- Walsh A. J., Hyland A. R., Robinson G., Burton M. G., 1997, MNRAS, 291, 261
- Walsh A. J., Burton M. G., Hyland A. R., Robinson G., 1998, MNRAS, 301, 640
- Walsh A. J., Macdonald G. H., Alvey N. D. S., Burton M. G., Lee J. -K., 2003, A&A, 410, 597
- Wiesemeyer H., Thum C., Walmsley C. M., 2004, 428, 479
- Wilson T. L., Walmsley C. M., Snyder L. E., Jewell P. R., 1984, A&A, 134, L7
- Wilson T. L., Walmsley C. M., Menten K. M. Hermsen, W., 1985, A&A, 147, L19
- Wood D. O. S., Churchwell E., 1989a, ApJ, 340, 265